The influence of grain size on the mechanical properties of Inconel 718

The influence of grain size on the mechanical properties of Inconel 718

LIU-IEI-TEK-A—13/01780--SE

Examiner: Prof. Johan Moverare
Supervisor: Jonas Saarimäki
Author: Muhammad Moiz

Department of Management and Engineering (IEI)
Division of Engineering materials
Linköping University
SE-581 83 Linköping, Sweden

Autumn 2013

Summary

In this thesis the influence of grain size on the mechanical properties of Inconel 718 has been studied. In718 is commonly used superalloy which has a relatively low cost but offer good mechanical properties. The research work was conducted from preparing two specimens of In718 that has been heat treated at different temperatures. The grain sizes were measured on both the specimens using Light Optical Microscope (LOM). The in-depth microstructural analysis was done using Scanning Electron Microscope (SEM) to study different phases and constituent elements. The mechanical tests, i-e tensile, creep, stress relaxation and hardness were also performed to investigate the response of In718 after heat treatment. Different techniques of SEM were used in this study. The mechanical test results show the deterioration of tensile strength and hardness while improvement of creep life with the increase of grain size. The stress relaxation results give inkling of the influence heat treatment on In718. The thesis work helps in better understanding the response of In718 at different temperature range, together with the constituent elements influencing different phases.

Abstract

The thesis work discuss about how the materials mechanical properties are influenced by the microstructure. The most common way of altering the microstructure of the material is by heat treatment. The mechanical properties that are of interest are strength, toughness, ductility, creep and fatigue. The material under consideration is widely used superalloy In718. Two different sets of specimens are heat treated at different temperatures and influence of heat treatment on the grain size is analyzed. In order to get better understanding of the grain size on mechanical properties, microstructural investigation was done using SEM. Efforts are made to understand the influence of different elements on the overall characteristic of the material. The tensile, creep and stress relaxation tests were conducted and the results were discussed.

Key words: Superalloys, microscopy, grain size

Preface

This thesis work is the conclusion of the Master's programme in Mechanical engineering (majoring in material science) at the Linköping University (LiU), Sweden. The thesis work has been conducted at the department of Management and Engineering (IEI) division Engineering materials. The thesis work is performed under the supervision of Jonas Saarimäki and examined by Johan Moverare. The aim of the thesis work is to understand and investigate the influence of grain size on the mechanical properties of the Nickel based superalloy; Inconel 718. The microscopy, which was done by grain size measurement using Light Optical Microscopy (LOM), and a more in-depth microstructural study was done by Scanning Electron Microscopy (SEM). Mechanical testing such as; creep, stress relaxation and hardness testing were performed at the end to strengthen the knowledge on macroscopic scale.

Acknowledgements

The author would like to express his sincere gratitude and respect to the examiner Dr. Johan Moverare for providing the opportunity for this thesis work, which has been both interesting and challenging. Appreciation and gratitude to Jonas Saarimäki, for having kept his office door open for open discussion and patience, with a smile on his face. The Engineering Materials division staff members especially, Research Engineer; Annethe Billenius in the engineering materials laboratory for technical discussions and assistance in using the Light Optical Microscopy (LOM) and hardness testing. PhD students Kang Yuan for using Thermo-Calc software for phase study and Zhe Chen for his assistance using the Scanning Electron Microscope (SEM) and discussing the results. Professor Sten Johansson for his expert reflections and suggestions on the SEM results, and finally administrator; Ingmari Hallkvist for providing the management support. The conducive environment provides opportunity of open discussion and feedback, that helped throughout the thesis period to improve my work and opportunity to expand my field of knowledge.

And last but not the least my ever supporting family and their unparalleled support and patience for believing on me.

Muhammad Moiz
Linköping, November 2013

Table of Contents

1. Notations

Specimen A	Specimen of Inconel 718 before heat treatment (as provided by the manufacturer)
Specimen B	Specimen of Inconel 718 after heat treatment (performed at the Engineering Materials lab at LiU)
In718	Inconel 718
Ni	Nickel
LOM	Nikon Metallurgical Light Optical Microscopy
SEM	Scanning Electron Microscope
SE	Secondary Electron
EDS	Energy Dispersive System
WDS	Wavelength Dispersive X-Ray Detector
EBSD	Electron Back Scatter Diffraction
ECCI	Electron Channeling Pattern
DLE	Dry Low Emissions
T_m	Melting temperature
CO_2	Carbon dioxide
CO	Carbon monoxide
NOx	Nitrogen oxide and Nitrogen dioxide
TET	Turbine Entry Temperature
CC	Combustion chamber
FCC	Face Centered Cubic (crystal structure)
TCP	Topological Closed Packed
ODS	Oxide dispersion strengthened
Co	Cobalt
Cr	Cromium
W	Tungsten
Mo	Molybdenum
Ru	Ruthenium
Re	Rhenium
Ta	Tantalum
e.g.	example
etc.	etcetera

min	minutes
BCT	Body Centered tetragonal structure
i-e	that is
Hf	Hafnium
SHT	Solution Heat Treatment
PH	precipitation or age hardening or Aging
ISO	International Organization of Standardization
HV	Vickers Hardness

2. List of figures

3. List of tables

4. Introduction

4.1 Introduction of research work

This thesis work is completion of the Master's programme, Mechanical engineering at Linköping University (LiU), Sweden. The thesis work has been performed at the division of Engineering materials, department of Management and Engineering (IEI). The objective was to investigate how different grain sizes influences the mechanical properties. The materials used for this study was Inconel 718, a Ni-base austenitic superalloy. Grain size measurements were done on two specimens A and B using LOM. SEM was used to investigate the different phases of specimen A and B. Tensile, creep and relaxation and hardness testings were all conducted in the engineering materials laboratory at LiU.

4.2 Background

The focus of the thesis was on the nickel based superalloy; In718. Although, there are different types of superalloys with their own unique characteristics and properties, but In718 stands apart, because of its good mechanical properties (yield strength up to 650 °C, impact and fracture toughness down to -40 °C) and good corrosion resistance [1,2]. The most important inherent property is its structural stability, which remain intact even close to its melting point [1].

4.3 Purpose of the thesis work

The thesis work was performed by investigating both on a macro and micro level, the influence of heat treatment on the mechanical

properties of In718. At the macro level, tensile, creep, relaxation and hardness tests were performed. On the micro level the grain morphology after heat treatment using LOM was investigated. Variations in chemical composition, were investigated by SEM. Figure 1, gives a holistic view of the influence of grain size on the major mechanical properties namely; tensile strength, crack growth, Low Cycle fatigue (LCF) and creep[1]. Figure 2, shows the influence of decreasing grain size on strength, toughness, weldability and ductility [1].

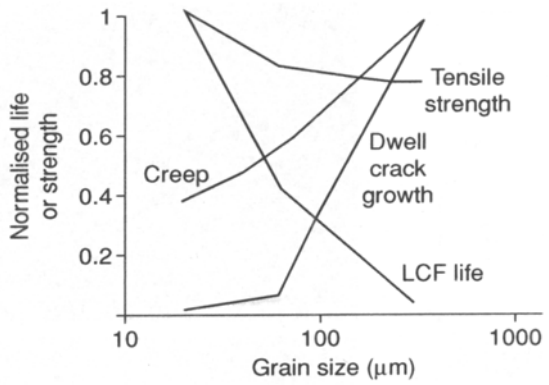

Figure 1(a): Schematic illustration of dependence of the mechanical properties on grain size [1]

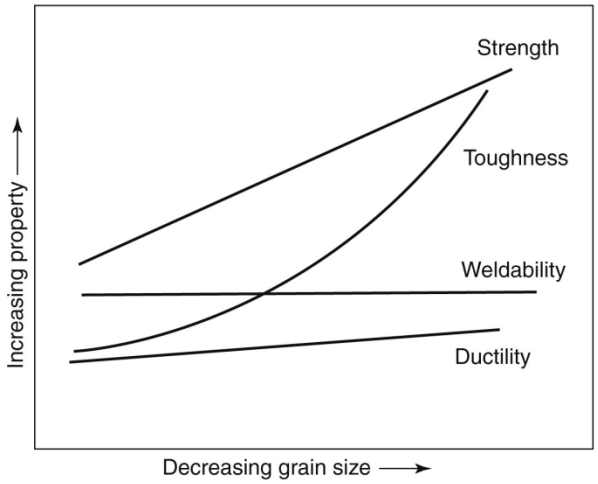

Figure 1(b): Influence of decreasing grain size on mechanical properties [15]

From figure 1(a) and 1(b), it is easily comprehended that the grain size increment has a direct relation to creep and dwell crack growth rate and inverse relation to tensile strength and LCF life.

5. Fundamentals of Superalloys

5.1 Introduction to superalloy

Superalloys, as the name suggest have characteristics that make them different from other materials. Usually consisting of multiple elements, modern superlloys may consist of more than 15 elements. This makes them a complex entity as compared to in the past where usually a single element tends to dominate. As we look in the past we realize that materials have played a substantial role in our civilization. These materials have had a direct or indirect influence on the culture, tradition, way of living, and doing business. With the advancement of science and technology that facilitates discovery of different new elements, there use seem to find their way from our daily life to applications in different industrial sectors. This not only facilitates our daily life but also revolutionize the way of looking broadly at things in new spectrums. Characterizing the elements based on their atomic number, chemical properties and electron configuration in the Periodic table, a combination of different elements provides unlimited possibilities of their applications. All elements in the Periodic table have their unique properties and characteristics that separate them from others. There are well defined limitations that constrain their use in specific areas of applications. Therefore no single material can be called "*The Material*" of choice for all applications. This gap has been filled by alloys and composites. Speaking about metals specifically, an alloy is a metal that contains two or more metals or non-metals [3]. They have relatively high strength, high stiffness, ductility or formability, and shock resistance based on their chemical composition.

Focusing the attention to power generation, the industrialization that mark the transformation of agrarian society to industrial society has brought social and economic development. This opens the door to technological innovation, which is primarily based on large scale

metal extraction and energy production. The power generation sector faces new challenges due to an increasing demand of energy production. These challenges will become even tougher when environmental issues such as sustainability and CO_2 footprints and emissions, are included in the design considerations. In order to address these issues more and more efforts are made primarily in developing metals alloys. That can have the ability to sustain not only high temperature but also retain their integrity with minimum (negative) environmental impacts. Gas turbines either land based or aero-engines; are the reason for the development of high temperature materials. According to [1], high temperature materials should possess the following characteristics;

I. "ability to withstand loading at an operating temperature close to its melting point".
II. "a substantial resistance to mechanical degradation over extended period of time".
III. "tolerance of sever operating environments".

These high temperature materials commonly called superalloys are developed to face the challenges of efficient energy demands but at the same time minimizing greenhouse gas emissions. Figure 2, shows the evolution of high-temperature capability of the superalloys over a 60 year period since their emergence in the 1940's. Since the 1940's, the evolution of materials and advance processes for turbine blading shows a holistic view of the progress in the development of superalloys. The creep performance taken as a criteria of at least 1000h at 137 MPa is plotted against the time (years) [1].

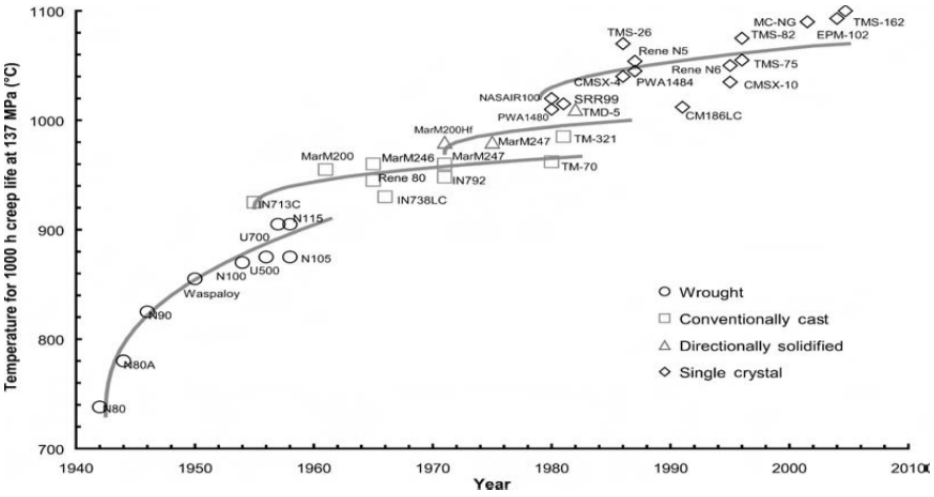

Figure 2: An overview of the development of superalloys (for turbine blade) and process development [1]

It has been shown in the literature that the development in the field of superalloys is basically fed by the gas turbine industry, therefore it is of utmost importance to understand the function of the various components in a gas turbine [4].

Figure 3(a): The Land-based gas turbine SGT-800 for power production, real life image [5]

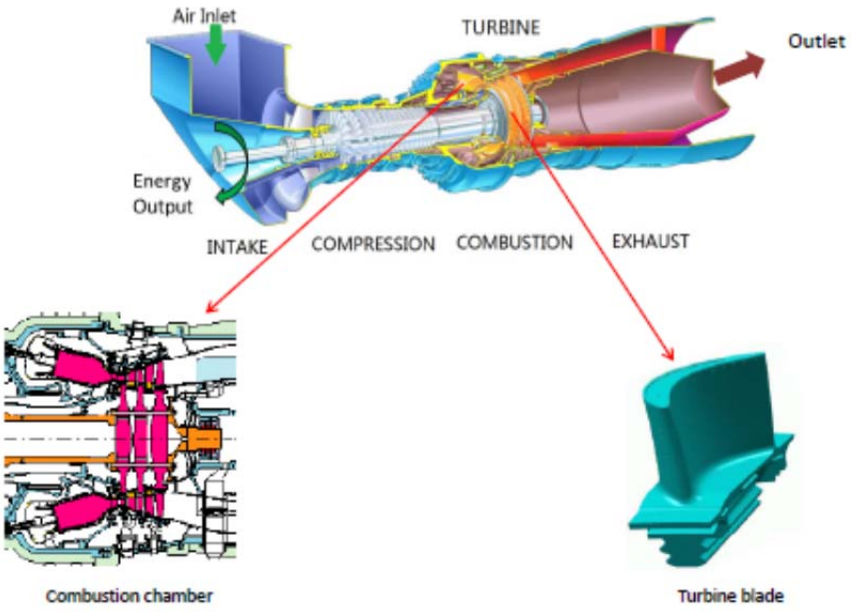

Figure 3(b): It shows a cross-section of SGT-800 and a close up of combustion chamber and turbine blade [5]

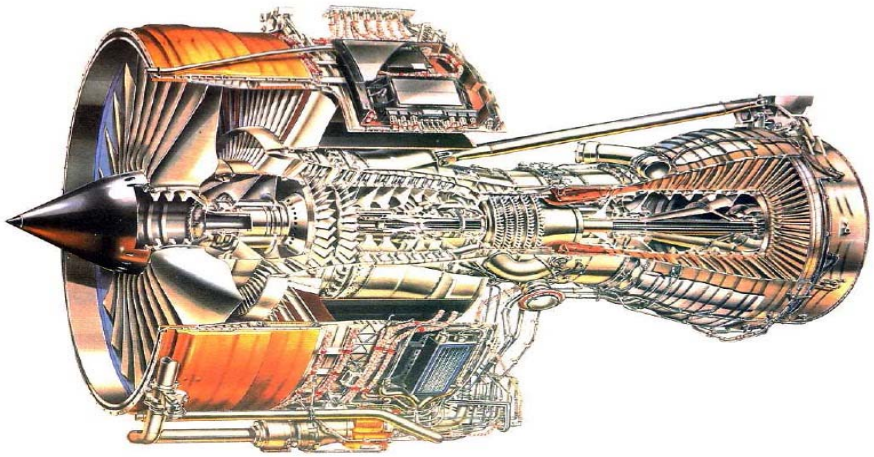

Figure 4(a): Rolls-Royce Trent 800 aero-engine [4]

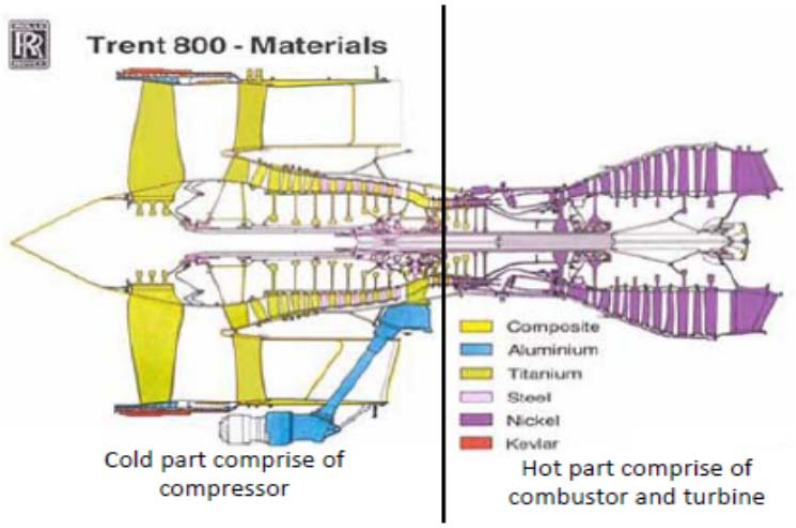

Figure 4(b): Rolls-Royce Trent 800 aero-engine with distribution of materials used at different sections [4]

Gas turbines are volume flow machines [6], the two broad categories of gas turbines are :

1) Land-based (standing/stationary), and
2) Aero/jet engine based (flying)

The major components of gas turbine are (irrespectively of the above mentioned categories):

a. Compressor: the compressor consist of alternating sets of rotating airfoils: rotors (blades) and stationary airfoils: stator (vanes). The compressor has variable guide vanes. The function of the compressor is to suck air from the environment and compress it in to the combustion chamber. Resulting in an increasing pressure ratio and enthalpy increase.

b. Combustion chamber (CC): the compressed air enters the combustion chamber where it is mixed with fuel and ignition

takes place. There are two different types. One is called "premixed combustion" where fuel and air are mixed before entering the reaction zone, used in Dry Low Emission (DLE) combustion systems. The second is called "non-premixed" combustion in which fuel and air is introduced separately [6].

c. Turbine: the hot gases enters the turbine and expand, resulting in an extraction of mechanical work required to drive the compressor, which is conducted by a shaft that connects the turbine to the compressor [1].

d. Exhaust: the gases after combustion find their way through the exhaust. Typical gas turbine emissions are carbon dioxide (CO_2), carbon monoxide (CO) and NOx (NO and NO_2).

There are different variants of gas turbines, depending on their use. Figure 4.2 shows the distribution of materials used in a Rolls-Royce Trent 800. The design of a gas turbine depends on if it is a land-based gas turbine or jet engine. The basic differences are the variation in thermodynamic cycles and the Turbine Entry Temperature (TET) which is usually constant for land based gas turbine because of fewer start-up/shut–down cycles as compared to jet engines where the TET can fluctuate during the whole flight cycle [1].

The hot parts in the combustor and turbine are critical in terms of thermal and mechanical loads and material used. When designing a gas turbine the main focus is placed on the TET. The reason why there is a steep increase in TET is that the efficiency of gas turbines are directly proportional to the TET and pressure ratio, which undoubtedly puts high demands on the development of new materials (superalloys) to fulfill the ever increasing TET demand.

Figure 5, shows the evolution of the TET capability for Rolls-Royce civil aero-engines from 1940 till 2010 [1]. It is obvious from the figure that the TET has increased nearly 700°C in about 60 years, which shows the level of interest and investment in the research and development of superalloys to enable operation temperatures close to their melting point without compromising the mechanical properties. From figure 5 it is also clear that the trend is ever increasing, which provide a conducive environment for the development of new techniques to satisfy the increasing TET requirement. But as the temperature reaches the melting temperature of the material, several phenomenon such as degradation of mechanical properties, creep, oxidation and corrosion starts to dominate. A number of different techniques have been developed to cope with these challenges. Since 1960, the interest for complex cooling techniques of turbine blades using computational fluid dynamics have been developed. From the end of 20^{th} century we have seen the development of thermal barrier coatings (TBC's), and the future promises development of new techniques towards achieving higher TET but at the same time safeguard the material integrity for long period of time. As a universal law, you have to lose something to gain some thing, the same rule applies when trying to increase the TET and pressure ratioas well. Increasing TET is a disadvantage as it means more heat input and simultaneously more cooling, but at the same time more work output which corresponds to high efficiency. This finally contributes to hotter exhaust. High pressure ratios will require more work input at the compressor stage, which is a disadvantage but at the same time will give more output work and require less input heat in the CC. This results in colder exhaust.

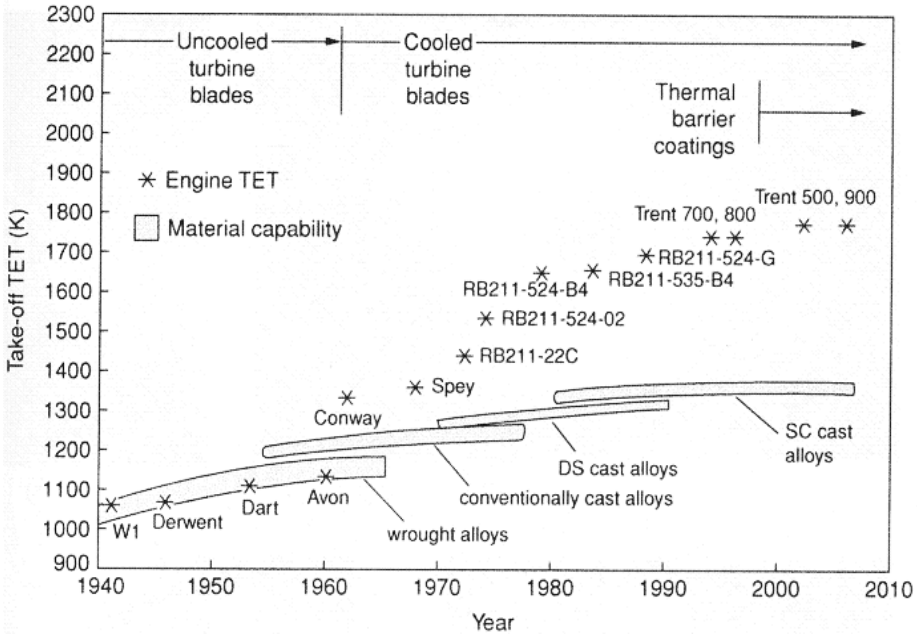

Figure 5: Rolls-Royce civil aero-engine TET increment with the passage of time [1]

5.2 Types of superalloys

There are numerous superalloys developed by different manufacturers, which found there applications in the aircraft industry, chemical plant equipment, power generation, nuclear power plants etc. They are available in cast (usually heat treated or otherwise processed) or wrought (often heat treated or otherwise processed) forms [7]. The chemical composition of each of them varies, based on the desired characteristics. The current superalloys are usually consist of 10 to 15 elements. But there are three main categories that are jointly called superalloys as mentioned below. They possess high level of temperature insensitivity or stability and are widely used as base materials for high temperature applications [1,8,9].

I. Nickel based
II. Iron – Nickel based, and

III. Cobalt based

These alloys are generally used at temperature above 450 °C, as at these temperatures ordinary steel and titanium alloys are losing their strengths, also corrosion is common in steels at this temperature [4].

I. **Nickel based superalloys**: The solid solution γ phase constitutes the Ni phase, which has a Face Centered Cubic (FCC) crystal structure [2]. Usually used when high strength is the required, for the temperature range of 1024 to 1371 °C [7]. They are a widely used and renowned group of austenitic alloys. The unique characteristic of this group of superalloys are their application without compromising their integrity close to their melting temperatures. Ni-base superalloys can be divided into three types:

- Solid solution strengthened alloys: which usually contains the following alloying elements; Fe, Co, Cr, Mo, W, Ti, Nb and Al [10,11]. Such as Haynes230 and HasteloyX. Among these Al, Cr, W and Mo are potential solid–solution strengtheners because of different atomic radius as compared to Ni [8]. They are more suitable for processing, for example weldability [9] and can also be manufactured into complex geometries from powders using laser melting techniques as described in [11].

- Precipitation (age) hardened alloys: usually contain AL, Ti, Ta and sometimes Nb that facilitate the formation of γ' and γ'' precipitates in the γmatrix [1,8,9]. Such as In718, 738, 939 and Waspalloy. From figure 6 [10], it is evident that precipitation hardened alloys possess higher strengths compared to solid solution

strengthened alloys and are widely used in high temperature applications [9,10].

- Oxide dispersion strengthened (ODS) alloys: alloys contain fine oxide particles of Y_2O_3 about 0.5 to 1% [11].

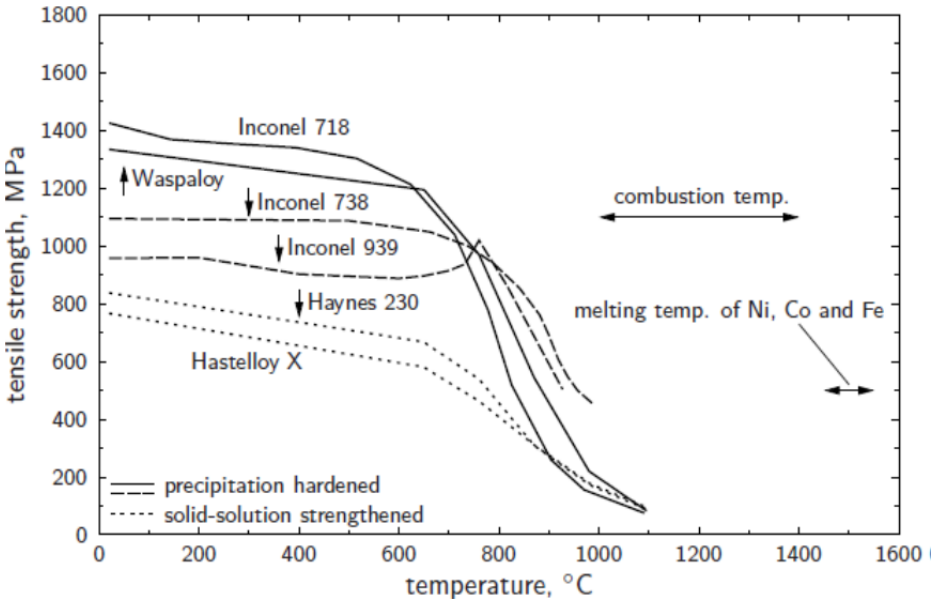

Figure 6: Tensile strength of superalloys at different temperature ranges [10]

II. **Nickel-iron superalloys:** The most important class of this group are those alloys that are strengthened by an intermetallic compound precipitation in an FCC matrix. The common precipitate is γ' [1]. Alloys such as In718, which has γ' and γ'' precipitates are classed as iron-nickel base because of their higher percentage of Fe, but are considered to be nickel based. Others superalloys in this group consist of stainless steel strengthened by solid-solution hardening [4]. They are

primarily used as a wrought material and are comparatively cheaper than Ni base alloys.

III. **Cobalt based superalloy:** are strengthened by the combination of carbides and solid solution hardeners. Cobalt crystallizes in the Hexagonal closed packed (HCP) crystal structure below 417°C, as shown in the figure 7 [12]. They possess excellent corrosion resistance at high temperatures (980-1100 °C) because of their higher chromium contents [15]. They possess better weldability and thermal fatigue resistance as compared to nickel based alloy. But cobalt-base alloys are more likely to precipitate undesirable sigma (σ) and Topological Closed Packed (TCP) phases. Depending on the application / composition involved it may be wrought or cast [7].

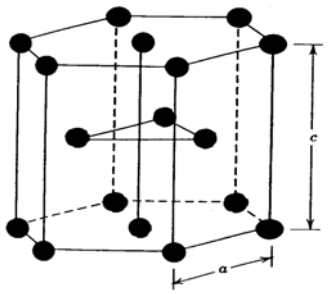

Figure 7: Hexagonal Closed Packed (HCP) crystal structure [12]

5.3 Physical metallurgy of nickel and its alloys

Nickel is the fifth most abundant element on earth and has a Face Centered Cubic (FCC) crystal structure as shown in figure 8 [12]. It belongs to the family of transition metals and exists in the form of five stable isotopes. Transition elements are often called transition metals (possess the properties of metals) or d-block elements, includes group 3-12 in the periodic table. The elements that are alloyed with Ni to form superalloys and the phases they contribute to also is mentioned in the figure 9 [1,14]. The melting temperature is ~ 1455 °C and has a density of 8907 kg/m^3 at room temperature. The characteristic that give Nickel excellent mechanical properties even at high temperature is its negligible yield strength / temperature sensitivity [15]. Another reason is that the FCC crystal structure that is both tough (toughness is the measure of resistance to fracture which is measured in units of energy [15]) and ductile because of the cohesive energy arising from the bonding provided by the outer electrons. Secondly, Ni is stable in its austenitic form from temperature to its melting point (i-e no phase transformation). Also low diffusion rate in FCC metals give good microstructural stability even at very high temperatures [1].

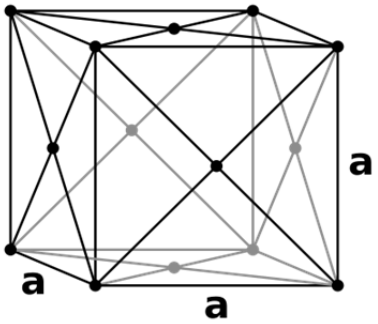

Figure 8: Face Centered Cubic (FCC) crystal structure [12]

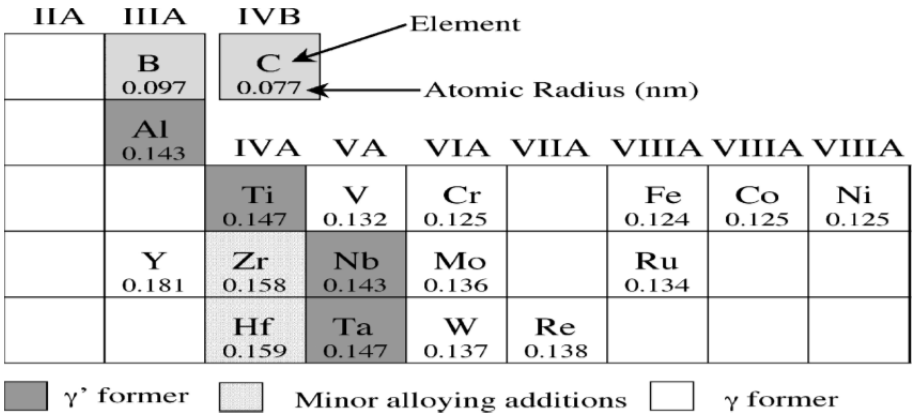

Figure 9: Representation of different alloying elements present in Ni base alloys[1,14]

Ni based superalloys belongs to the family of austenitic nickel-chromium based superalloys that typically contains 80% Ni and 20% Cr. Several alloying elements are included in different percentages depending on the need to achieve better mechanical properties. Ni-based alloys are usually strengthened by precipitation (age) hardeners, they may be wrought or cast depending on the application / composition involved. The composition of some Ni base alloys are given in table 1 [2], to give an idea about the complexity of these alloys, which from their inception in 1940's consisted mainly of 80% Ni and 20% Cr [16].

Alloy	Ni	Co	Fe	Cr	W	Mo	Al	Ti	Nb	Ta	Si	C	B
Haynes 230	57[a]	5[b]	3[b]	22	14	2	0.3	–	–	–	0.4	0.1	0.015[b]
Hastelloy X	47[a]	1.5	18	22	0.6	9	–	–	–	–	1[b]	0.1	0.008[b]
Inconel 738	61.4[a]	8.5	–	16	2.6	1.75	3.4	3.4	0.9	1.75	–	0.17	0.01
Inconel 939	47.3[a]	19	0.5[b]	22.5	2	–	1.9	3.7	1	1.4	0.2[b]	0.15	0.01
Inconel 718	52.5	1[b]	18.4[a]	19	–	3.1	0.5	0.9	5.1	–	0.35[b]	0.08[b]	0.006[b]
Waspaloy	58[a]	13.5	2[b]	19	–	4.3	1.5	3	–	–	0.15[b]	0.08	0.006

[a] balance
[b] maximum

Table 1: Composition some prominent Ni-based alloys [10]

The modern complex superalloy composition is due to unique phase chemistry and structure. The microstructure consists of different phases. The important ones such as gamma phase (γ), gamma prime (γ′), gamma double prime (γ′′) , delta phase (δ) and various carbides and borides are explained below.

- The gamma phase (γ): The gamma phase is the matrix phase of nickel-based superalloys in which the other phases reside. It exhibits a FCC crystal structure and its composition mainly consist of Ni with other elements such as Co, Cr, Mo, Ru, Re, and Fe [1,16,17].

- Gamma prime (γ′): forms the precipitate phase, which is usually coherent with the γ-matrix and is the main strengthening precipitate in nickel based superalloys. Similar to the γ phase γ′ have an ordered FCC crystal structure. γ′ mainly consist of Ni, Al, Ti, and Ta i-e $Ni_3(Al,Ti)$ [1,16,17].

- Gamma double prime (γ′′): is a strong coherent metastable precipitate with a body center tetragonal (BCT) structure, it is the primary strengthening precipitate [1].The γ′′ unit cell precipitate i-e Ni_3Nb consist of Ni and Nb is shown in figure 10 [1], is usually found in Ni-Fe superalloys. At higher temperature γ′′ become unstable and can transform into δ phase [18,19].

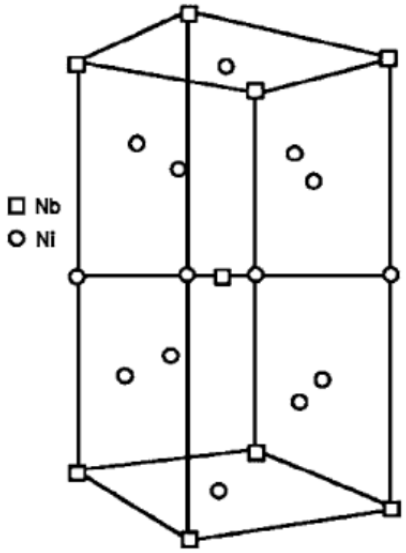

Figure 10: The unit cell of γ″precipitate [1]

- Delta phase (δ): is a non-hardening precipitate usually present at grain boundaries. The loss of hardening is due to depletion of γ″[16,19]. The structure is orthorhombic and the δphase improves the creep rupture and grain boundary sliding resistance. It is composed mainly of Ni, Nb and Ti [16,18].

- Carbides and borides: Carbide usually forms when carbon reacts with Ti, Ta and Hf and result in MC carbides. Where M represents elements such as Cr, Mo, Ti, Ta, or Hf. The MC carbides break-down during service to other species, such as $M_{23}C_6$, M_6C, M_7C_3, and M_3B_2. These decomposed compounds usually reside in theγ grain boundaries [1]. Borides are found in superalloy in the form of M_3B_2, having a tetragonal unit cell. Which is also present in grain boundaries and improve the creep rupture resistance of superalloys [9].

- Other phases: For example TCP, μ, σ, and laves etc. are present in the form of plates and needles. Under some conditions these can result in lower rupture strength and increase the creep rupture strength [1,9]. Although it is not desirable to have these compounds during service/operations.

6. Experimental procedure

In the conducted study, the nickel based superalloy In718 is investigated. The specimens have been manufactured from cylindrical solid bars of In718 along the longitudinal axis, as shown in figure 11. The specimens were fabricated according to the specification stated in appendix A.

Figure 11: Overview of the specimen manufactured from the In718 bar

The chemical composition was obtained by Electron Back Scatter Diffraction (EBSD) detector and the composition is given in table 2. The chemical composition from the manufacturer can also be found in Appendix A. Although in Appendix A, the manufacturer has mentioned 19 constituent elements but in this study only 11 elements are considered because of their significant proportion and their possible contribution in defining the mechanical properties ofIn718. To clarify Niobium (Nb) which is also called Columbium (Cb) is mentioned with both symbols to avoid confusion.

Aluminium	Cobalt	Iron	Cromium	Vanadium	Titanium	Niobium	Molybdenium	Tunsten	Tantalum	Nickel
Al	Co	Fe	Cr	V	Ti	Nb (Cb)	Mo	W	Ta	Ni
0.60	0.44	18.19	18.53	0.09	0.97	6.10	3.56	0.11	0.29	51.02

Table 2: The Composition of In718

The experimental procedure follows the following sequence, mentioned in table 3.

	Standard heat treatment	**Self conducted heat treament**
	Specimen A	Specimen B
Step 1	Solution heat treatment ~ 960 °C for 2h	Solution heat treatment ~ 1050 °C for 2h
Step 2	Aging: 720 °C for 8h	Aging: 720 °C for 8h
	620 °C for 8h	620 °C for 8h
Step 3	Grain size measurement using Light Optical Microscopy (LOM)	Grain size measurement using Light Optical Microscopy (LOM)
Step 4	Microstructure study using SEM	Microstructure study using SEM
	delta phase (δ)	delta phase (δ)
	γ"	γ"
Step 5	Hardness testing (Vickers-HV*)	Hardness testing (Vickers-HV*)
Step 6	Tensile testing	Tensile testing
Step 7	Creep 550 °C/1000 MPa	-
Step 8	Stress relaxation testing 550 °C / 0.8% applied strain	Stress relaxation testing 550 °C/ 0.8% applied strain

*HV= Vicker's number

Table 3: The Experimental procedure followed during this study

7. Microscopy

7.1 Heat treatment and etching

Heat treatment is the most widely used process most often used to achieve the desirable characteristics, as explained by [7].

- Reduce the stress level
- Provide mobility of atoms to redistribute alloy elements
- Promote grain growth
- Promote recrystallization of grains
- Dissolve phases
- Produce new phases, owing to precipitation from solid solution
- Provide a possibility for a surface chemistry change
- Forming new phases by introducing foreign atoms.

Heat treatment processes mainly aim towards impart desirable characteristic for the material; such as good mechanical strength at elevated temperature, oxidation and corrosion resistance. In this research work solution heat treatment (SHT) and precipitation or age hardening (PH) has been done. Both of them are mentioned in some detail below.

Solution heat treatment

"*It is heating of an alloy to an appropriate temperature, holding it at that temperature long enough to cause one or more constituents to enter into a solid solution and then cooling it rapidly enough to hold these constituents in solution. Subsequent precipitation heat treatments allow controlled release of these constituents either naturally (at room temperature) or artificially (at higher temperatures)*" [20].

Most solution heat treatments often soften or anneal [7]. And the alloys that are strengthened by SHT are called solution strengthened alloy. Elements in solid solution usually increase yield and tensile strength, other possibilities to increase strength is having finer grains [21].

Precipitation or age hardening (aging): They are done in order to bring out the desirable strengthening precipitates and control other secondary phases. They include carbides, borides, TCP etc.The aging process increases hardness and strength but at the cost of reduction in ductility[3].

These heat treatments are then followed by chemical process for example metallographic etching. It is technique that is widely used to highlights on microscopic features like grains, grain boundaries, inclusions, impurities and even phases [22]. The etchants used in this research are hydrochloric acid (HCl) and oxalic acid ($H_2C_2O_4$) in a ratio of 50:50. These etchant's are used to create contrast between elements in the In718 specimen by corroding some of those elements [22]. In order to visualize them simple microscope will not be of any help so Light Optical Microscope (LOM) will help in providing such magnification where above mentioned features can be observed. Figure 12, shows Nikon metallurgical Light Optical Microscope (LOM) with magnification lenses of 5X, 10X, 40X, 60X, and 100X used for LOM.

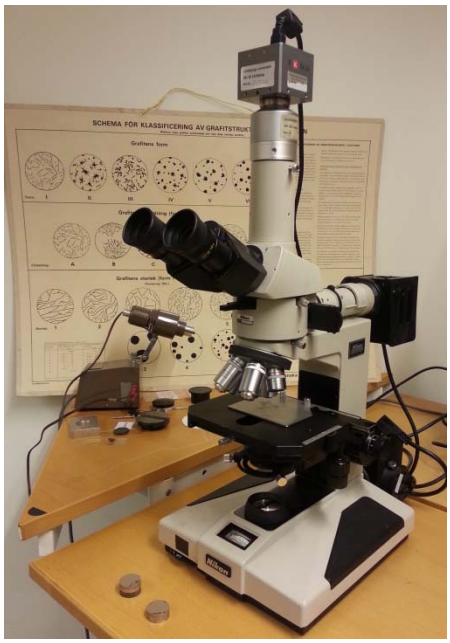

Figure 12: Nikon Metallurgical Light Optical Microscopy (LOM)

7.2 Microscopy and Grain size measurement

The grain size plays a significant role in achieving the desired characteristics for example creep, tensile strength, Low Cycle Fatigue (LCF), and crack growth as shown in figure 1 [1]. In order to investigate the above mentioned mechanical properties and their relation to grain size a careful preparation of the test specimen was done.

The crystalline solids are an amalgamation of many crystals, usually called polycrystalline. Each and every crystal is called a grain. The demarcation between grains are called grain boundaries [21]. The morphology of the grain boundaries are directly related to the heat treatment conditions [7]. Grains are often irregularly distributed throughout the material. The mechanical properties of metals are strongly dependent on grain size [3,7]. At room temperature, generally

as the grain size decreases the strength of the alloy increases while ductility decreases [1,7]. Grain size measurements were performed on both of the specimens A and B. A sequential metallurgical preparation process is required to examine the grain structure after the heat treatment has been done. The following processes are performed in sequential order:

I. Grinding
II. Polishing
III. Etching

Grinding was done in three steps using Silicon Carbide (SiC) emery paper, SiC 500 (30 μm), SiC2000 (10 μm), and SiC-4000 (5-6 μm) for 3-5 minutes (min). Polishing was done using 3μ Dur (Nylon cloth plate) for 15 min, 1μ Mol (cotton and nylon cloth plate) together with green lubricant for 25 min,0.25μ Nap (fiber plate) together with green lubricant for 25 min, , Master Met™ (Non-crystallizing colloidal Silica polishing suspension) on Chem cloth for 5 min, and water polishing for 30 s on another Chem cloth. Etching was performed using Hydrochloric acid (HCl) and Oxalic acid ($H_2C_2O_4$) in a ratio of 50:50. After the sample preparation process the microstructure of the specimen was investigated using Light Optical microscopy (LOM) with a magnification of the eyepiece 5X, 10X, 40X, 60X, and 100X.

As mentioned in table 3, In718 specimens A and B are solution heat treated at about 960 °C for 2 hours and at 1050 °C for 2 hours respectively, followed by aging at 720 °C for 8 hours and subsequently at 620 °C for 8 hours for both of the specimens. Figures 13-17 shows an overall view of the variation of grains sizes keeping the magnification constant while comparing specimen A and B.

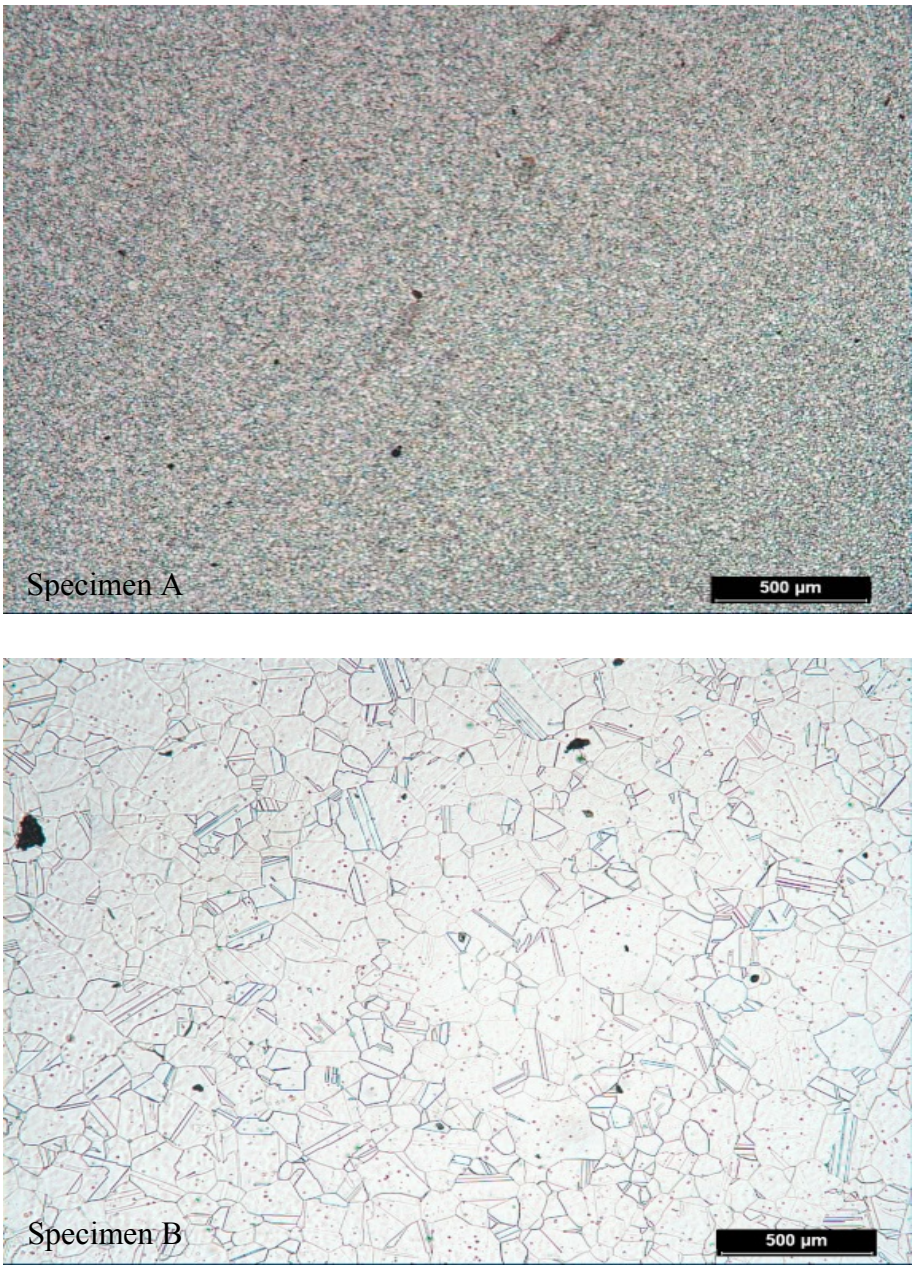

Figure 13: LOM image at 5X magnification after heat treatment and etching of specimen A and B

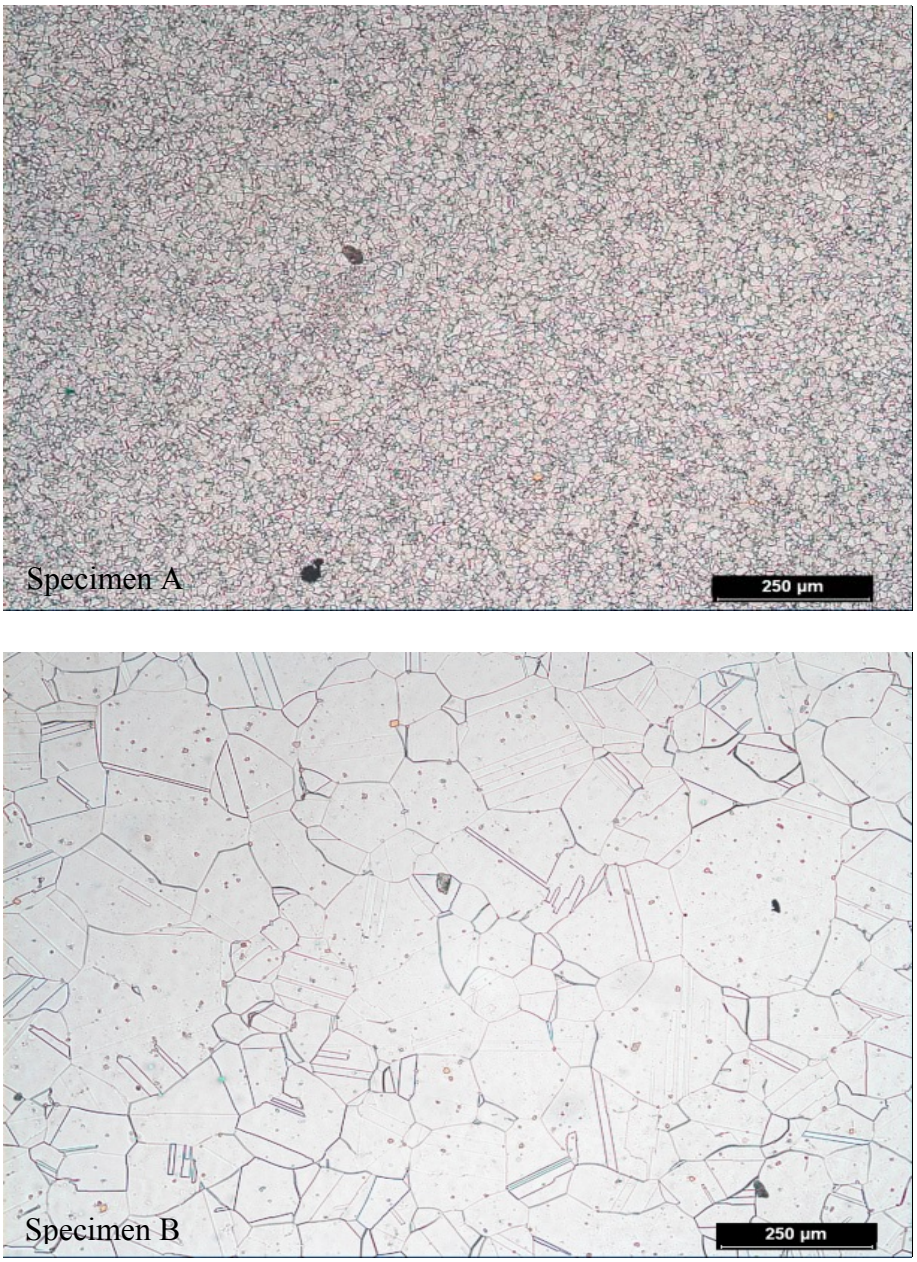

Figure 14: LOM image at 10X magnification after heat treatment and etching of specimen A and B

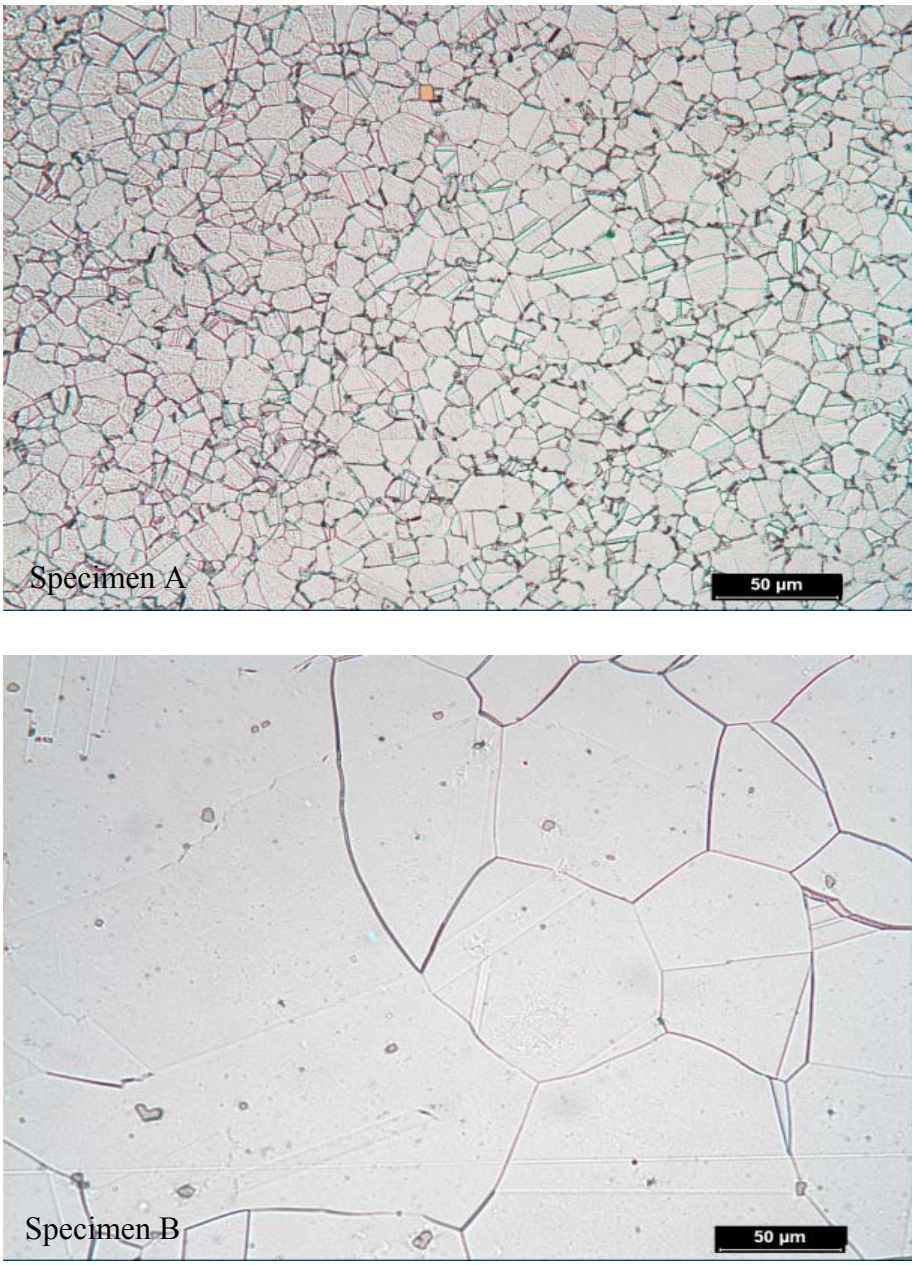

Figure 15: LOM image at 40X magnification after heat treatment and etching of specimen A and B

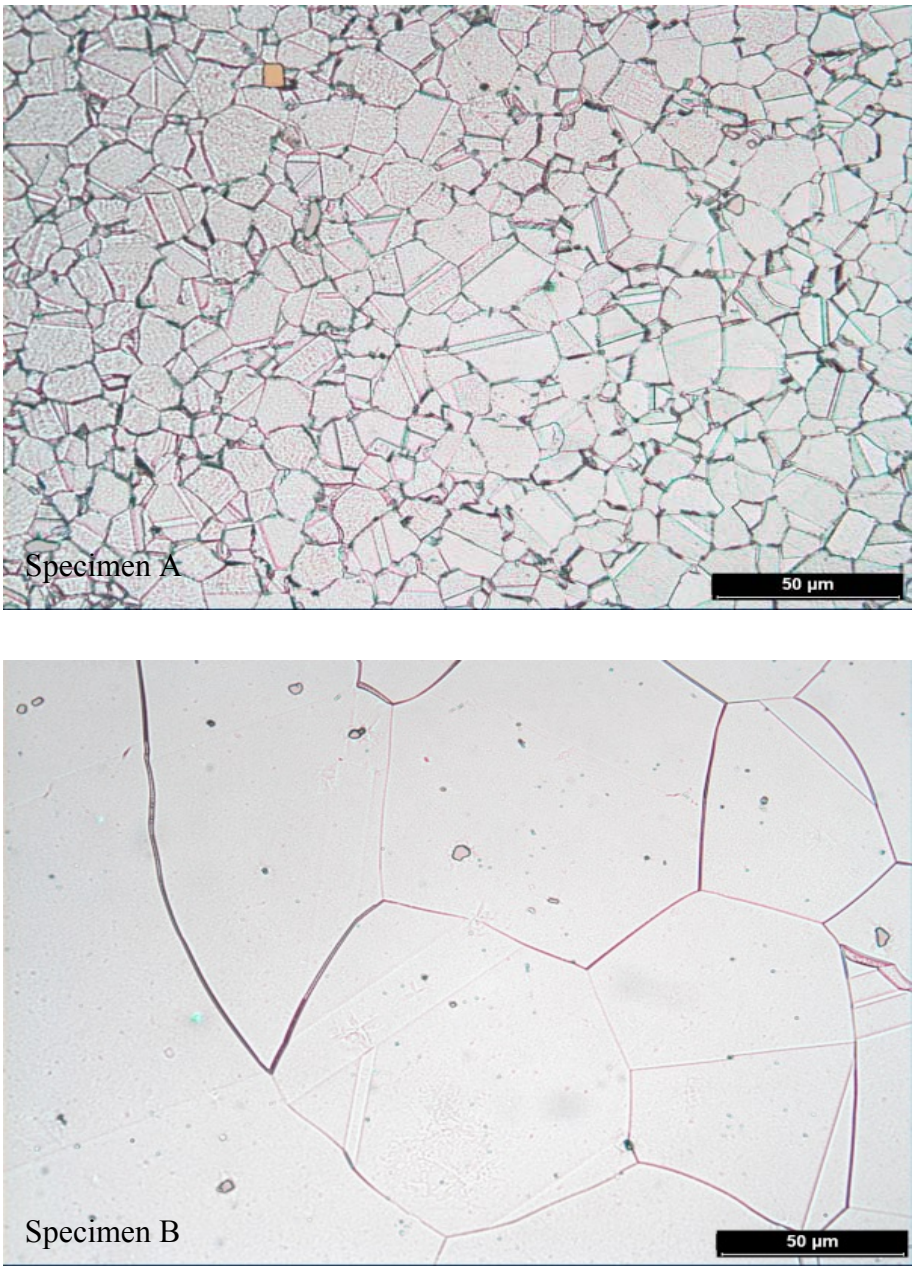

Figure 16: LOM image at 60X magnification after heat treatment and etching of specimen A and B

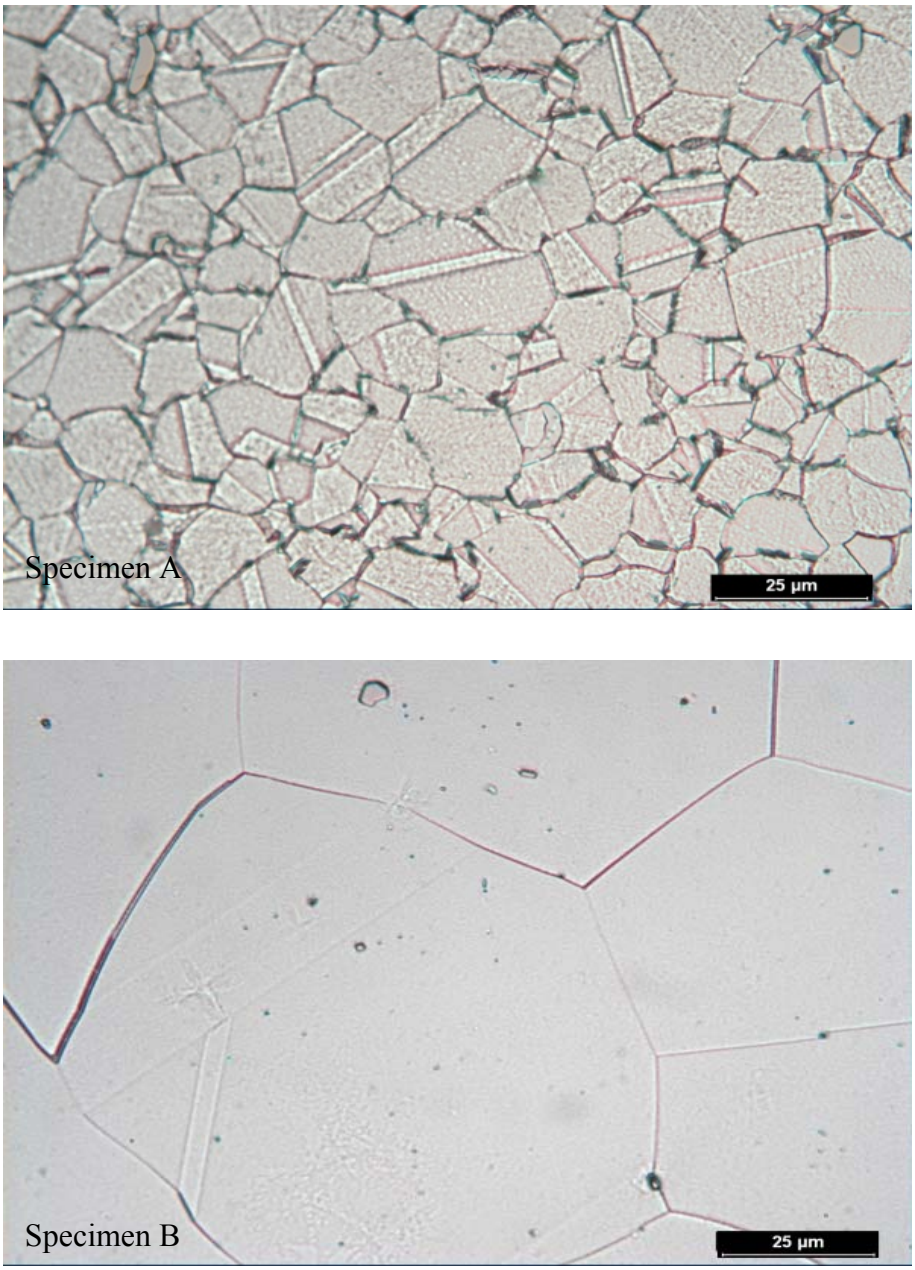

Figure 17: LOM image at 100X magnification after heat treatment and etching of specimen A and B

The average grain size measurement have been done following the ASTM E112-12 and ISO 643 standards [22,23]. There are different methods for grain size measurement; for example the intercept method, planimetric methods, and the comparison method. The Intercept and Planimetric methods are applicable for determining average grain size while comparison method is not applicable for the measurement of individual grains [22]. Therefore the intercept method was selected to conduct average grain size measurement. Since the measuring procedure is basically dependent on geometry it can be applied on any metals or alloys [22]. ASTM E112-12 purely deals with the determination of planar grain size, that consider grain as 2-dimensional entity. After careful observations, the grain size of specimen A was calculated to be ~ 9 μm which is in conjunction with the manufacturer specification mentioned in Appendix A. The average grain size after heat treatment was ~ 88 μm.

A number of interesting observations were done while measuring grain sizes. One is the observation of twins. In order to discuss it further it is good to give a short background of twins or deformation twins and the difference between slip and deformation twins. As both terms are used interchangeably and sometimes give the impression of different sides of the same coin, they are completely different. Slip is the primary mechanism by which plastic deformation takes place [21]. Twining in a pair of grains appears when the arrangement of atoms in one of the grains can be generated by a reflection across the common plane [24]. The prominent difference between a slipped versus a twinned crystal is the external shape change resulting from these deformations [15]. The slip is about a simple translation across the slip plane, that it's rigid portion of the solid moves relative to the other without deformation. A twinned body on the other hand undergoes a significant shape change without any translation along the twinning plane [7,15]. Figure 18(c), shows twinning of an FCC system.

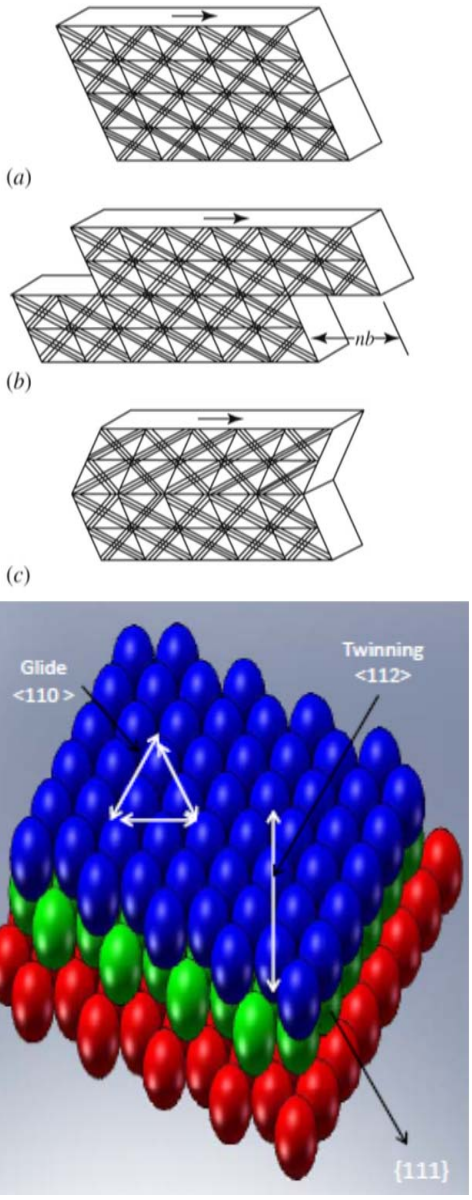

Figure 18: Shape change in solid cube due to plastic deformation. (a) Undistorted cube; (b) slipped cube that is translated to a distance nb; (c) twinned cube revealing reorientation within twin [6], (d) FCC twinning system [25]

So putting it simple the twinning process has triggered the lattice rotation while the slip occurs by translation and the orientation of the slipped cube remains intact [15]. Twins have a unique orientation relationship; the boundaries that separate the twins have a low energy per unit volume [24]. An important thing to remember is that the twinning crystal orientation is rotated without distorting of the crystal structure [25].

After clarifying the difference between slip and twinning, it is important to differentiate *deformation (mechanical) twins* versus *annealing twins*. As the name indicates deformation twins are basically generated by plastic deformation of single grains and there is a large influence of strain energy in its formation, as twin thickness increases with decreasing shear strain [15]. While annealing twins are due to inherent plastic deformation, that means that no shape change takes place [15,24,26]. Annealing twins basically nucleate during thermal processes [27]. The driving force of twinning is the net reduction of grain boundary energy that is related to twinning [26]. The apparent difference between the above mentioned twins is that deformation twins are point and lens shaped while annealing twins are flat and not pointed [24], while the interface consist of both coherent and non-coherent segments [15]. The specimens that were considered were from a forged bar, for grain size measurements and has not undergone any deformation processes except the inherently preexisting plastic deformation due to forging. Basically the annealing twins were formed or become more obvious during heat treatment as a result of recrystallization and growth of new grains. In the LOM, annealing twins were easy to identify in both of the samples, as shown in the figure 19(a) and 19(b). Twin bands exhibit a change in contrast, since the lattice reorientation within the twins cause the incident light to be reflected away from the lens of LOM [15]. The twin band marking will persist even after re-polishing and etching of the specimens, since they are purely connected to the re-orientation of the lattice and have nothing to do with the surface feature (slip) [15].

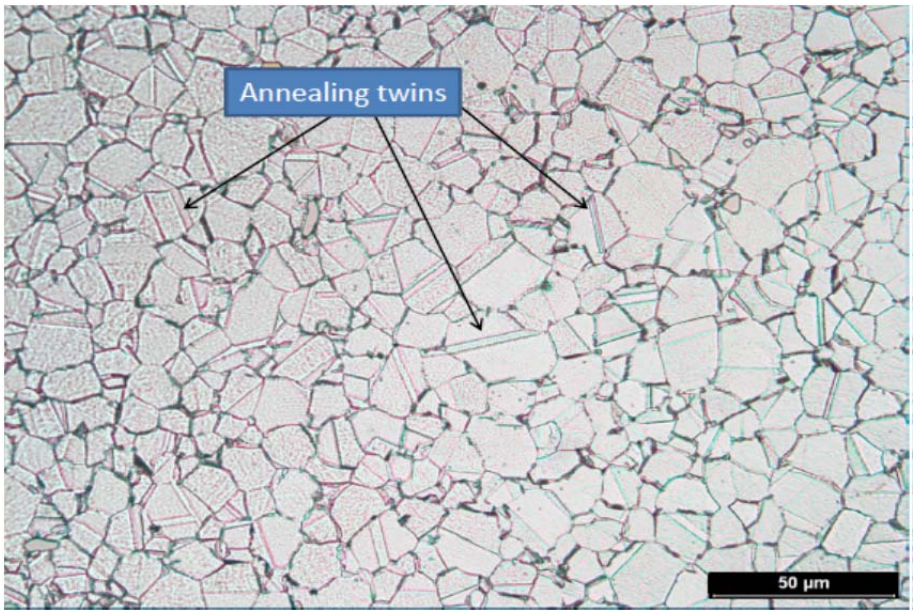

Figure 19(a): LOM image at 60X magnification showing annealing twins in specimen A

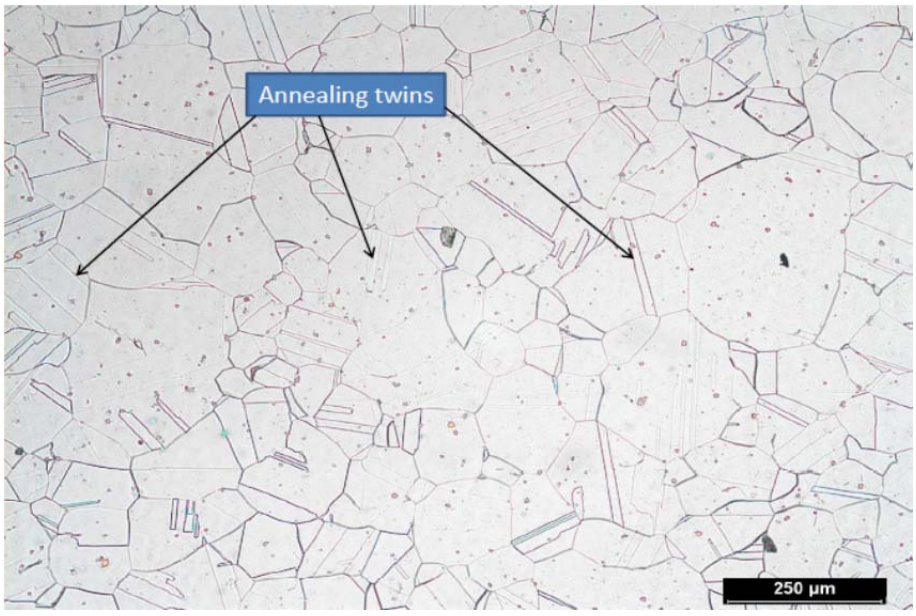

Figure 19(b): LOM image at 10X magnification showing annealing twins in specimen B

The annealing twin formation basically proceeds in two steps, initiation and propagation and has been investigated more in [28].

An investigation was also conducted considering the twins as grain boundaries and not considering twins as grain boundaries. The motivation was to see how it influences the average gain size. Figure 20, shows the grain size distribution in specimen A, with and without twins considered as grain boundaries. Figure 20(a) shows the positive or right skewed distribution with a mean grain size value of ~ 8 µm. Figure 20(b) shows more close to normal distribution with a mean grain size value of ~ 9 µm, which is inline with the grain sizes previously calculated.

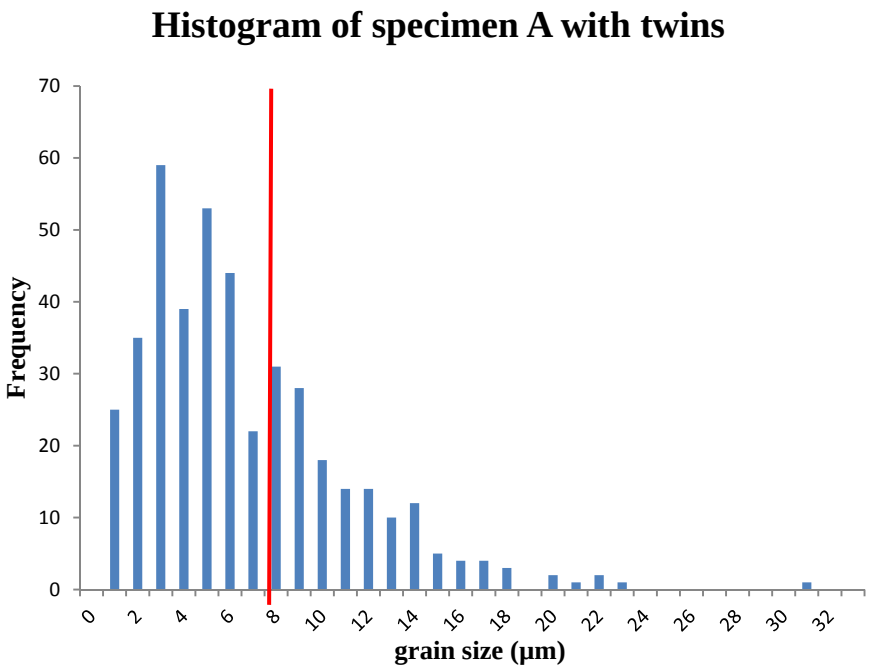

Figure 20(a): Distribution of grain size of specimen A considering twins as grain boundaries

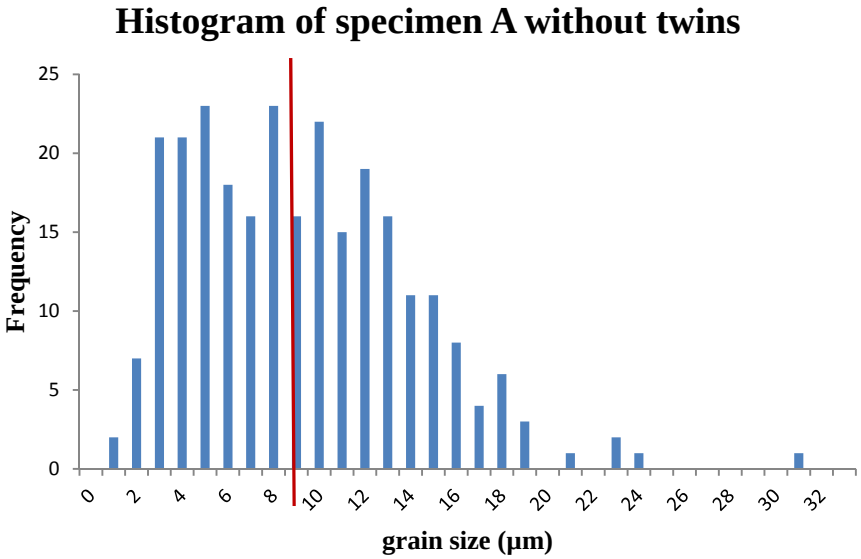

Figure 20(b): Distribution of grain size of specimen A neglecting twins as grain boundaries

The same analysis has been done on specimen B. Figure 21(a) shows the positive or right skewed distribution with a calculating average grain size of ~ 58 µm. Figure 21(b) shows a close to normal distribution with calculating average of ~ 88 µm, which is inline with the grain sizes previously calculated.

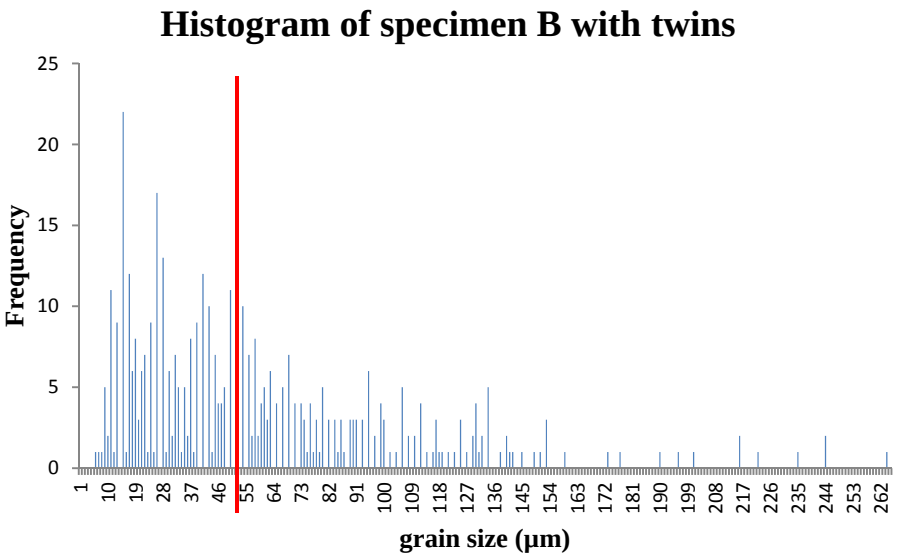

Figure 21(a): Distribution of grain size of specimen B considering twins as grain boundaries

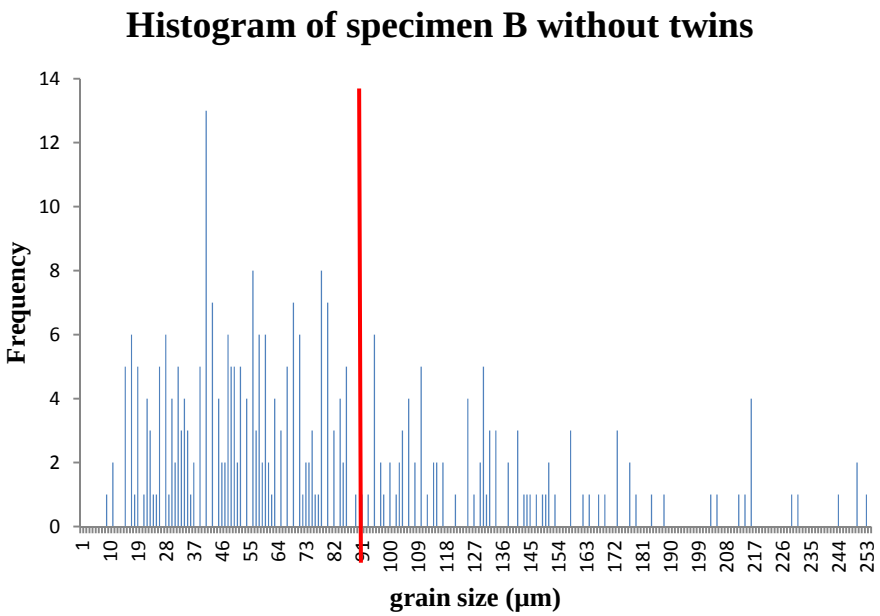

Figure 21(b): Distribution of grain size of specimen B neglecting twins as grain boundaries

Therefore the conclusion is that twins should not be considered as grain boundaries as they are parts of the grains and not the grain themselves [24,28], which is confirmed from the investigation of twins.

7.3 Study of different phases

In order to dig more into detail, rather than analyzing grains superficially, a microstructural study has been performed using different SEM related techniques like Secondary Electron (SE) and Backscattered electron (BSE). The Scanning Electron Microscopy (SEM) model Hitachi SU-70, with a resolution of 1 nm, having an analytical capacity with EDS, WDS and EBSD has been used to conduct the investigation.

Figure 22: Overall view of Hitachi SU-70 Scanning Electron Microscope (SEM) in LiU engineering materials laboratory

SEM is a relatively new technique, which facilitate in sample imaging (morphology-study of shape, and topography-study of crystal quality and visualizing defects) used basically for surface topographic studies where the surface of the sample is investigated in three dimensions with both high resolution and high magnification. Better focusing and smaller wavelength of electrons enables to achieve higher magnification (>10^5) better resolution (10-50 Å) and give an increased depth of field (2 µm-1 mm) [30]. The resolution is several orders of magnitude greater than an LOM. [29]. Specimen information is obtained from the interaction between a primary electron beam and a material [29].

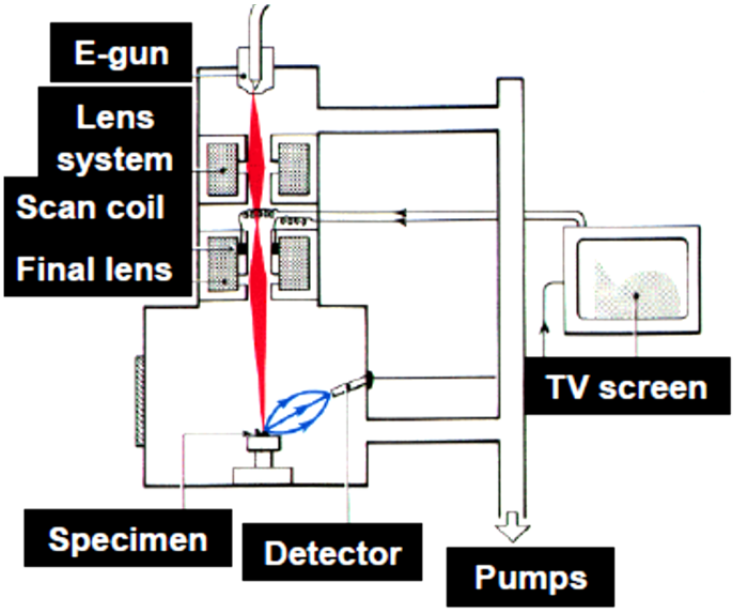

Figure 23: Schematic diagram of SEM [30]

The basic principle is that a specimen is scanned by an incident electron beam and the electrons and / or photons emitted from the surface of the specimen are collected, detected and analyzed at the same time. The lenses in the microscope condense and de-magnify the electron beam to form a focus spot on the surface of the specimen. The whole analysis requires high vacuum conditions [30]. The electron and photons generated in the excitation volume carry different information form the specimen under observation [30].

Any type of interaction between the electron beam and the sample can result in contrast. The resolution depends on what kind of interaction is used. The imaging using different kinds of interaction between the electron beam and the sample is called the imaging modes of the SEM. The most common imaging modes with short explanation of the information that they carry is given [30]:

- **Secondary electrons (SE)**: information related to topography, magnetic and electric field.
- **Backscattered electrons (BSE)**: information related to topography, crystallography and composition.
- **Absorbed specimen current**: information related to topography and composition.
- **Cathode luminescence**: information related to electronic and optic.
- **Induced conductivity**: is used to study isolators
- **Electron channeling patterns (ECP) and Electron Backscattered diffraction (EBSD)**: information of crystal structure of a specimen.

In the conducted investigation the imaging modes considered are SE, BSE, and EBSD, a description is given below [30]:

Secondary electrons (SE): depends on topography and is the most common contrast mode is Secondary electron (SE) detection where a

high resolution of ~ 5 Å can be obtained. This corresponds to the magnification in the SEM in the vicinity of (100X to 200000X) [29]. Prominent features are:

- Three dimensional appearance
- Sensitive to orientation
- High resolution imaging

Back Scattered Electron (BSE): also called topographic or compositional imaging. "*BSE are high energy electron produced bythe elastic collision of incident electron beam with the electron cone of the sample atoms"* [30]. Prominent features are:

- Provides elemental composition variation as well as surface topography
- Large escape depth compared to SE results
- Mapping possibility of individual elements
- Detectors that combine topography and composition signals

Specimen A

The chemical composition of Specimen A after standard heat treatment is shown in table 2.Figure 24 shows an overall view of the elemental composition of specimen A. BSE imaging technique is used to investigate elemental composition together with their distribution. As can be seen from the figure 24, there is a distribution of black dots and white dots, although white dots seem to be distribute more evenly. Upon improving the magnification the neddle shape δ (Ni_3Nb) phases are visible, that are transgranular and intergranular. Transgranular δ phases are those that grows through the grain in a fairly ordered way, as shown in figure 26. While intergranular δ phases grows mainly in the grain boundaries of the material, as shown in figure 25. The

chemical composition of δ phase was found out using an X-ray detector of which the results are shown in table 4. As described earlier, δ phase which is a non-hardening precipitate composed mainly of Ni, Nb and Ti [16,18], in this case it is Ni_3Nb. The influence of δ phase on mechanical properties ofIn718 is not well defined [31]. In In718 γ′ and γ″ phases are responsible for the high temperature strength [31].

Ni	Al	Fe	Cr	Ti	Nb	Mo	C
56.59	0.32	9.07	9.17	1.82	19.01	2.71	1.30

Table 4: Chemical composition of **δ** phase

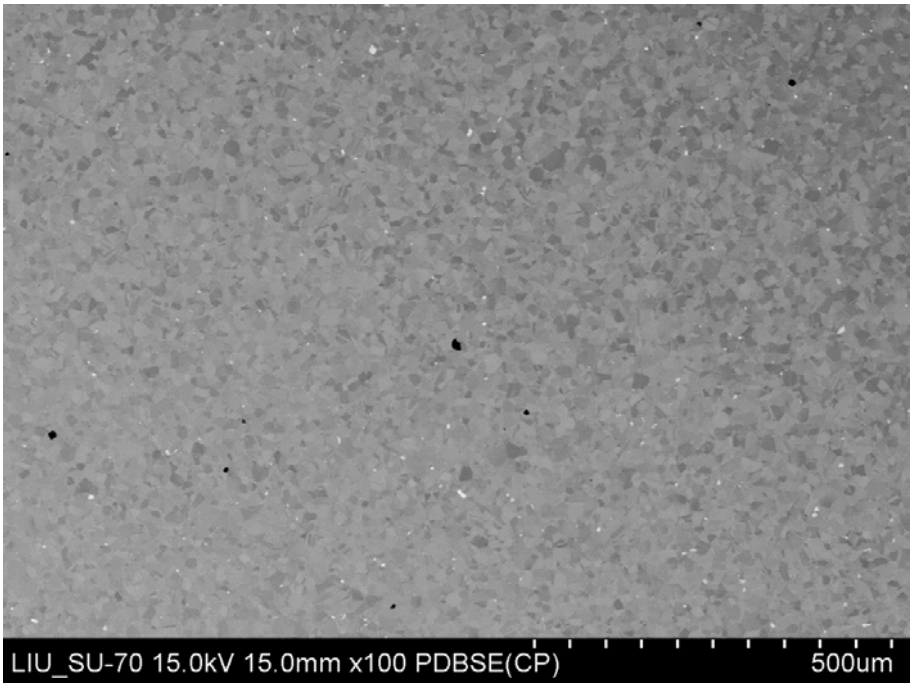

Figure 24: Overall BSE imaging of specimen A

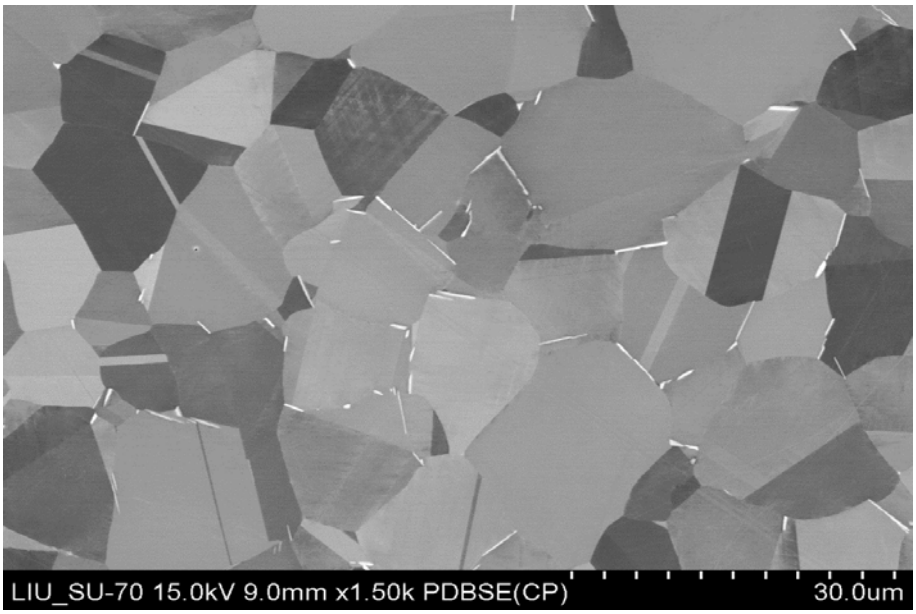

Figure 25: BSE imaging of specimen A showing mainly intergranular δ phase

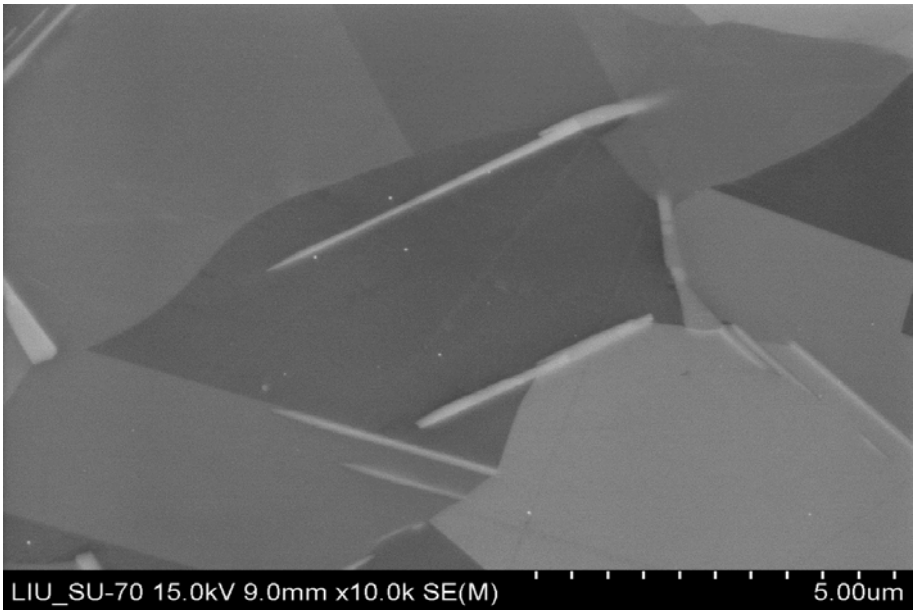

Figure 26: BSE imaging of specimen A showing transgranular needle shape δ phase

A chemical composition of white dots and black dots are found out using X-ray detector, given in the table 5 and 6 respectively. It is found out that the white dots are basically NbC and black dots are TiN.

Al	Cu	B	Co	Fe	Cr	V	Ti	Nb(Cb)	Mo	W	Ta	Ni	N	Si	Mn	C
0.01	0.10		0.04	0.31	0.35	0.03	6.59	82.81	1.85	0	0	1.09		0.59	0.05	6.18

Table 5: Chemical composition of white dots (NbC) in specimen A

Al	Cu	B	Co	Fe	Cr	V	Ti	Nb(Cb)	Mo	W	Ta	Ni	N	Si	Mn	C
0.04	0.16		0	0.30	0.46	0.27	72.07	9.39	0.36	0	0	0.76	16.06	0.12	0.01	

Table 6: Chemical composition of black dots (TiN) in specimen A

Figure 28 highlights the NbC and TiN in the overall view taken from the BSE, and figures 29 and 30 are the magnified versions of them.

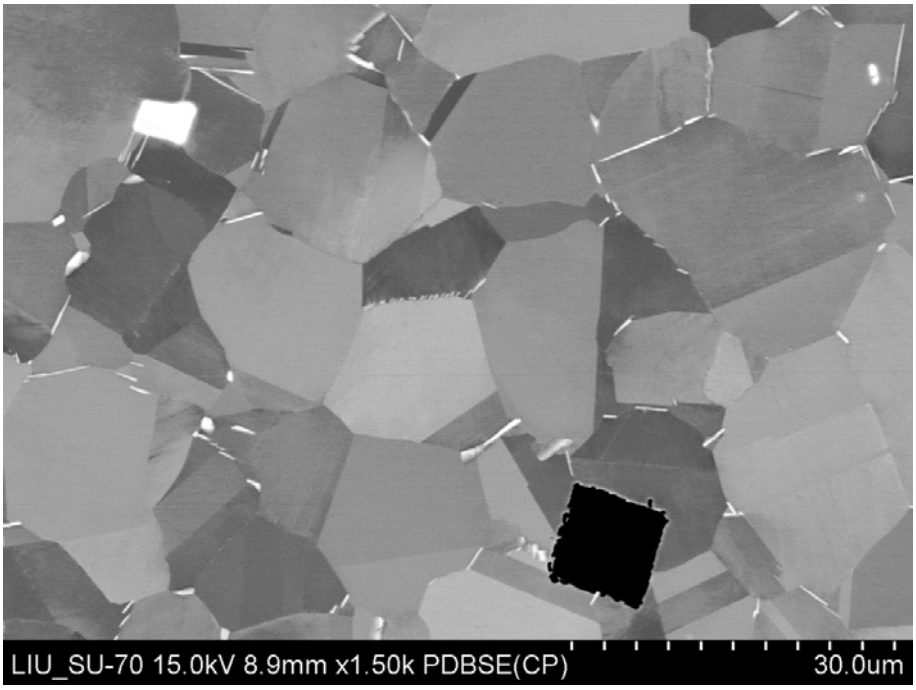

Figure 27: BSE imaging of specimen A showing white and black dots

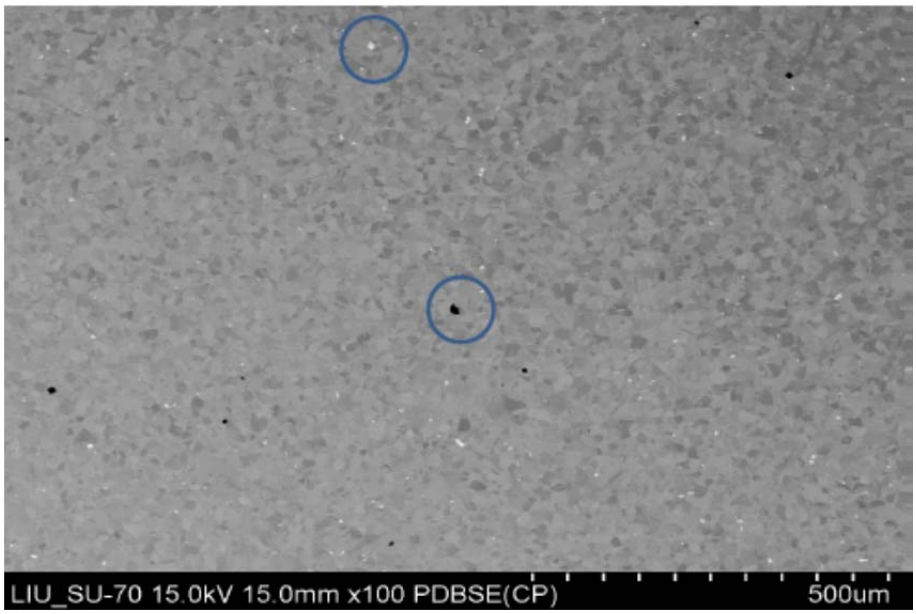

Figure 28: Overall BSE imaging of specimen A, showing NbC and TiN

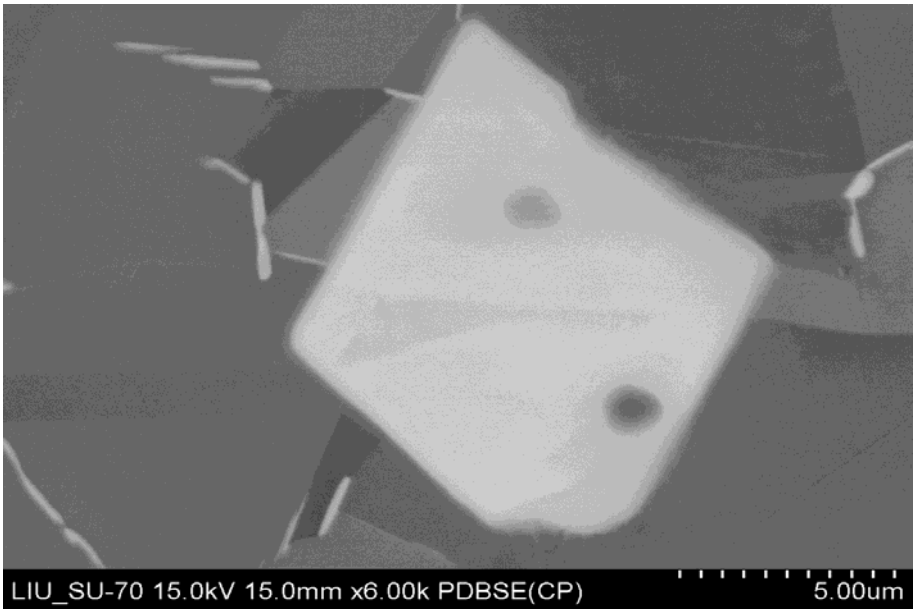

Figure 29: BSE imaging of magnified version of NbC as shown in fig.28 of specimen A

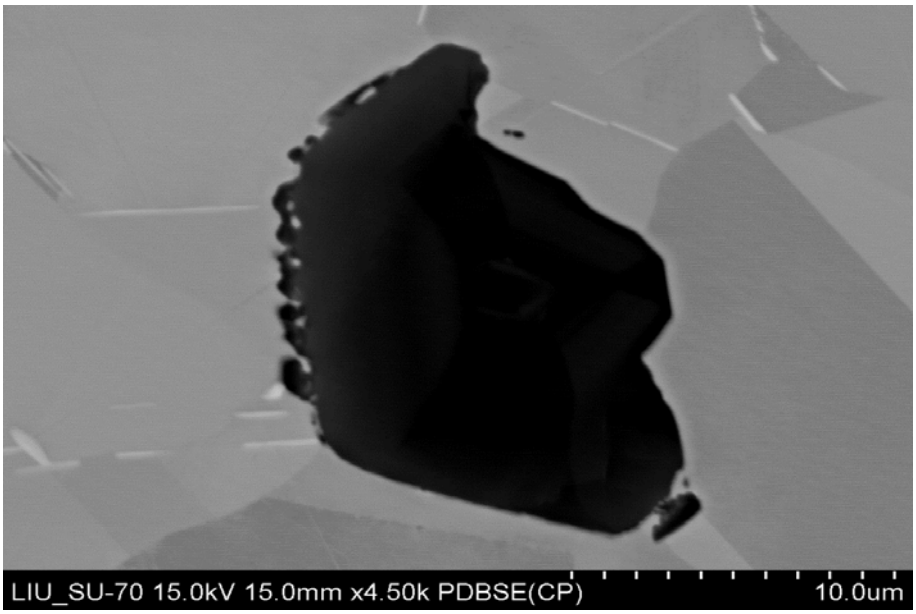

Figure 30: BSE imaging of magnified version of TiN as shown in fig.28 of specimen A

Figure 31, shows the γ″ phase of specimen A using BSE.

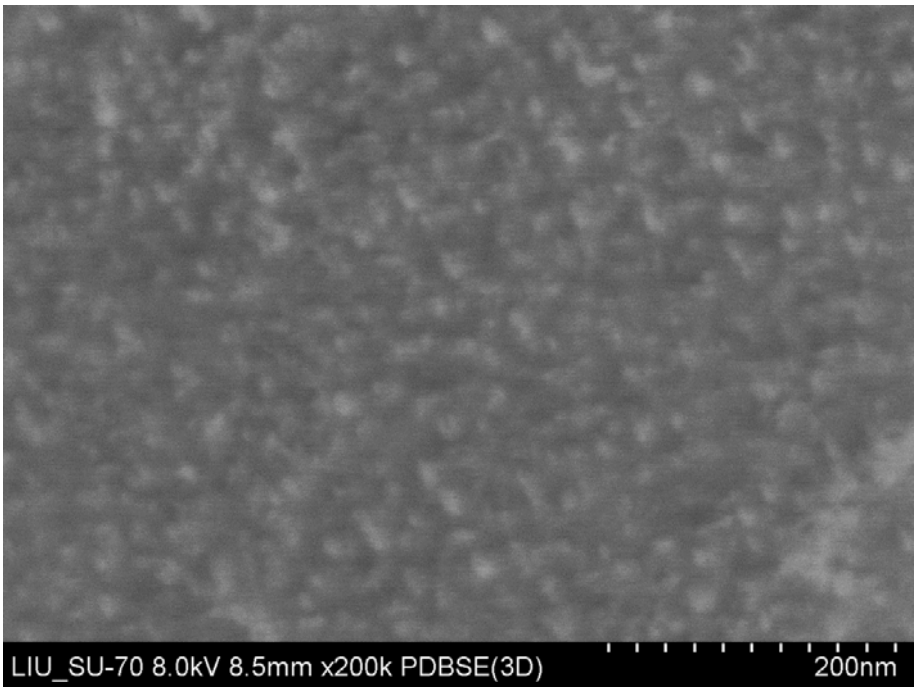

Figure 31: BSE imaging of γ′′ phase detected in specimen A

Specimen B:

The chemical composition of Specimen B after standard heat treatment is shown in table 7. Figure 32 shows an overall view of specimen B. BSE imaging technique is used here also to investigate elemental composition together with their distribution. As can be seen from the figure 32, the size of the grains has been increased substantially. There are distribution of black dots and white dots, although the size of them also increased. The interesting thing to observe in specimen B is that δ phase has not been observed. The chemical composition of NbC and TiN are shown in table 8 and 9 respectively. The chemical composition does not change much after heat treatment.

Al	Cu	B	Co	Fe	Cr	V	Ti	Nb(Cb)	Mo	W	Ta	Ni	N	Si	Mn	C
0.63	0.01		0.62	18.15	18.51	0.08	0.94	6.11	3.52	0.06	0.31	50.87			0.18	

Table 7: Composition of In718 in specimen B

Al	Cu	B	Co	Fe	Cr	V	Ti	Nb(Cb)	Mo	W	Ta	Ni	N	Si	Mn	C
0.01	0.07		0.02	0.41	0.39	0.09	6.52	82.35	2.59	0	0	1.05		0.47	0.04	5.99

Table 8: Chemical composition of white dots (NbC)in specimen B

Al	Cu	B	Co	Fe	Cr	V	Ti	Nb(Cb)	Mo	W	Ta	Ni	N	Si	Mn	C
0.02	0.09		0	0.27	0.53	0.33	69.35	13.16	0.54	0	0	0.80	14.77	0.12	0.03	

Table 9: Chemical composition of black dots (TiN) in specimen B

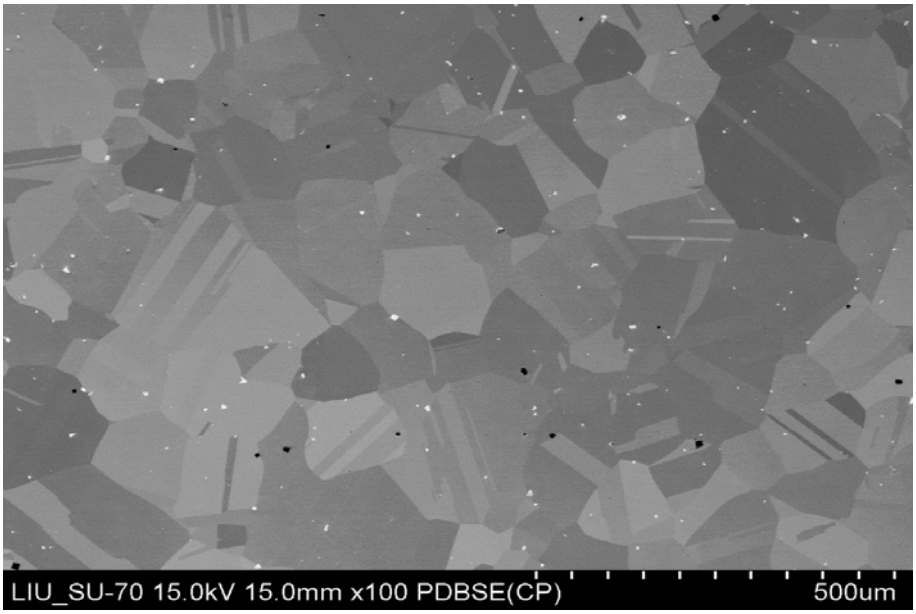

Figure 32: Overall BSE imaging of specimen B

Figure 33 highlights the NbC and TiN in the overall view taken from the BSE, and figures 34 and 35 are the magnification of them. Figure 36, shows the γ'' phase of specimen A using BSE.

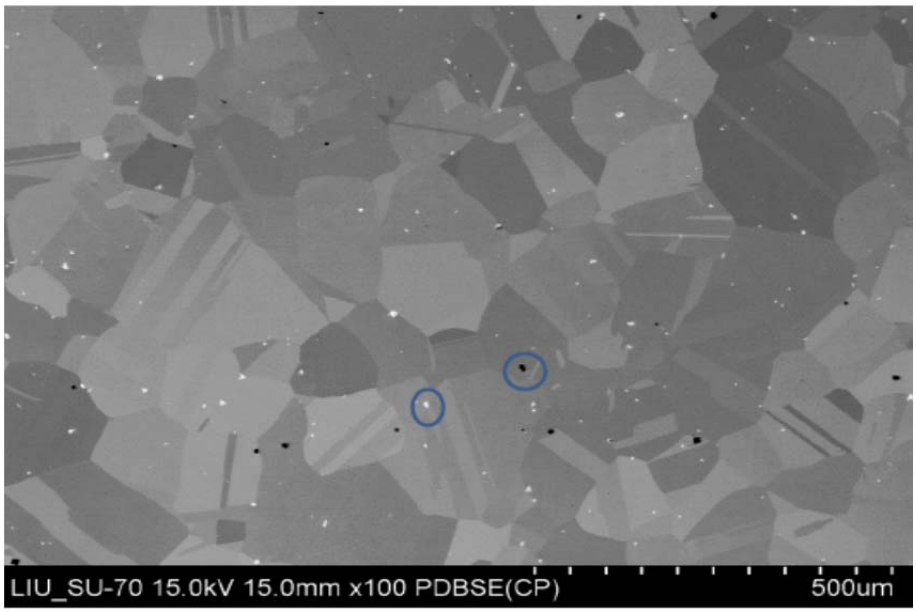

Figure 33: Overall BSE imaging of specimen B, showing NbC and TiN

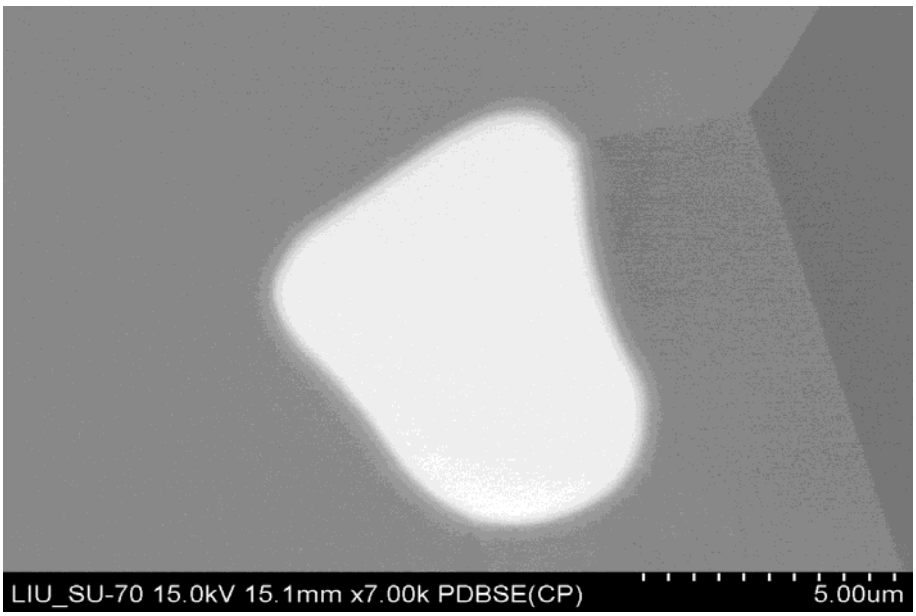

Figure 34: Overall BSE imaging of specimen B, showing NbC

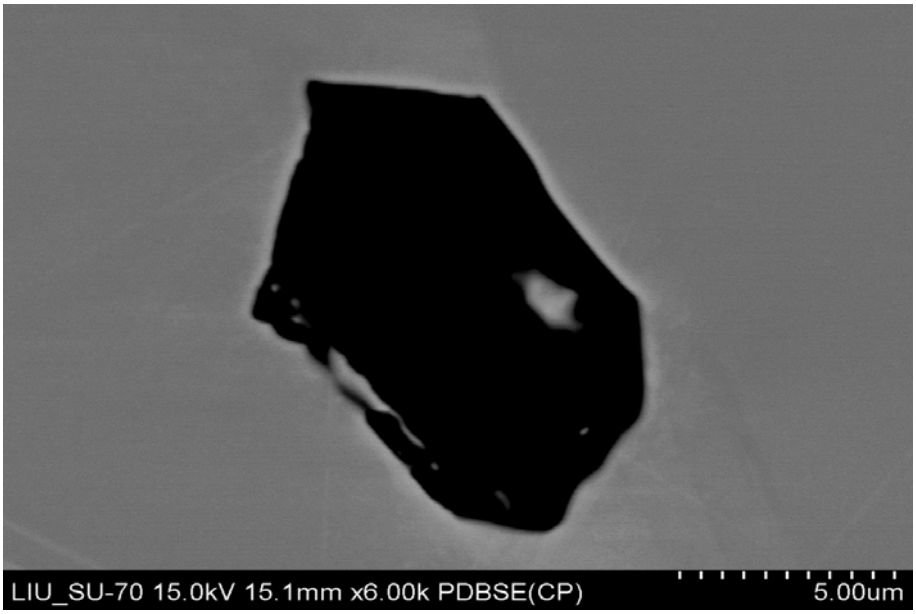

Figure 35: Overall BSE imaging of specimen B, showing TiN

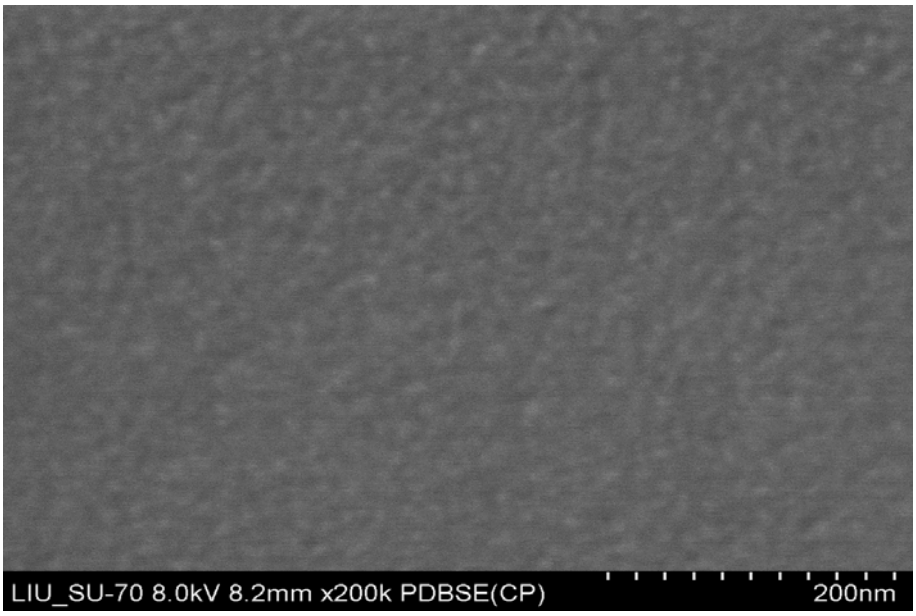

Figure 36: BSE imaging of γ'' phase detected in specimen B

7.4 Discussion

The BSE investigation shows some interesting results. γ′ phase has not been observed in both samples. As mentioned in section 5.3, γ′ mainly consist of Ni, Al, Ti, and Ta i-e $Ni_3(Al,Ti)$. As shown in table 2 and 7, the percentage of Al and Ti is very low, therefore the formation of γ′ is neglibile. The δ phases that were observed in the specimen A, after heat treatment have dissolved into the matrix . The absence of δ phase/precipitate at the grain boundaries improve the elemental homogeneity at the grain boundaries and increase the intergranular stress corrosion cracking resistance of the material. Also a notable point is that the absence of δ phase at the grain boundaries decreases the crack propagation rate of the material [32]. The formation of δ phase in specimen A during heat treatment can influence the morphology of the grain boundaries [31]. Since the aging time for specimens A and B are only 16 h in total, γ′′ in both the materials are observed. It was observed by [33], that long aging times during the service temperature, γ′′ decompose into stable δ (Ni_3Nb) phase. There is a close correlation between δ precipitate growth kinetics and evolution of Nb content in the matrix.

8. Mechanical testing

8.1 Tensile testing

The tensile strength of both the specimen has been observed at 550 ºC at strain rate of 2E 10^{-3}, and the engineering stress vs engineering strain are plotted as shown in figure 37. The results are inline what has been shown in figures 1 and 2. The grain size that increases because of heat treatment results in reduction of strength of In718. The tensile strength that was mentioned in material certificate data sheet (see Appendix B) is 1448 MPa. This was measured at 20 ºC (or room temperature) by the manufacturer. The tensile strengths obtained for specimen A was ~ 1230 MPa and that of specimen B was ~ 1010 MPa, both at 550 ºC. The variation is understandable as tensile strengths were measured at different temperatures. While the fracture in specimen A takes place before specimen B.

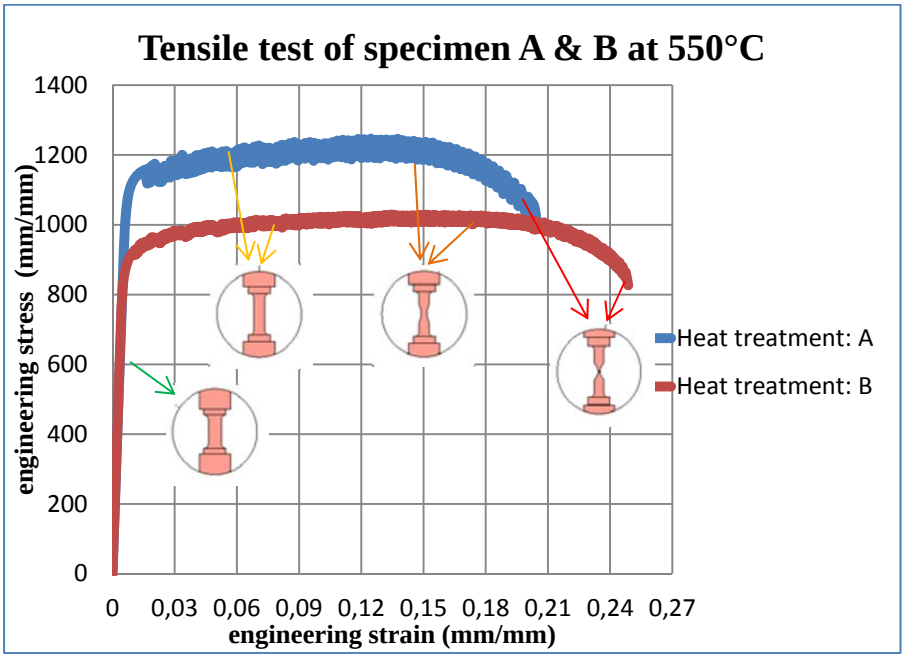

Figure 37: Stress strain plot of specimen A and B are shown

Figure 38: Specimens Of In718 before and after tensile test of specimen A and B shows ductile failure

8.2 Creep testing

The creep is an increasing in plastic deformation under constant mechanical loading, often at elevated temperature. May result in large deformation and/or rupture [34]. Creep is an irreversible time-dependent deformation typical for metals [15]. The creep test that was performed on specimen A and B were isothermal constant load creep test, in which strain is recorded as a function of time. The test was conducted at 550 ºC at 1000 MPa. From figure 40, for simplicity the creep curve is divided into three regimes [15].

- Stage I : transient or primary creep stage where strain rate decreases and microstructural hardening take place
- Stage II: steady state creep stage, which indicate a stable structure and a dynamic balance between hardening and

softening process. the strain rate remains constant or minimum.

- Stage III: tertiary stage involves in an increase in strain rate, weakening due to metallurgical instabilities.

In Stage I, In718 undergoes a period of transient response where strain rate decrease, followed by stage II which is a steady state that dominate major portion of materials life and finally stage III where final failure occurs as the creep rate increases. The phenomenon's that interact by varying creep response are strain hardening and strain softening (recovery) processes, which strongly affect the overall strain rate of the material at a given temperature and stress [15]. Figure 39 shows the setup for the creep test on the Kappa 50 DS mechanical testing machine.

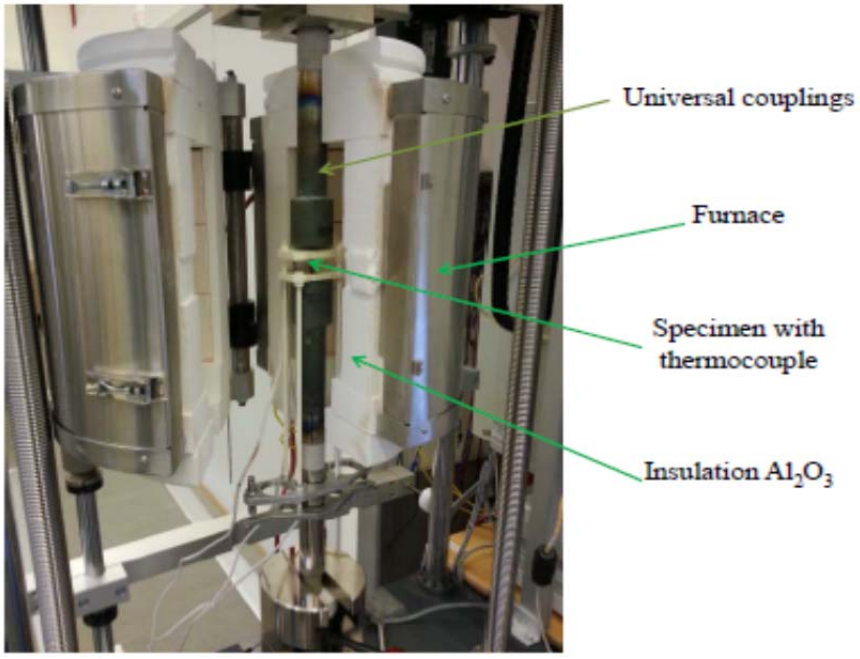

Figure 39: kappa 50 DS mechanical testing machine

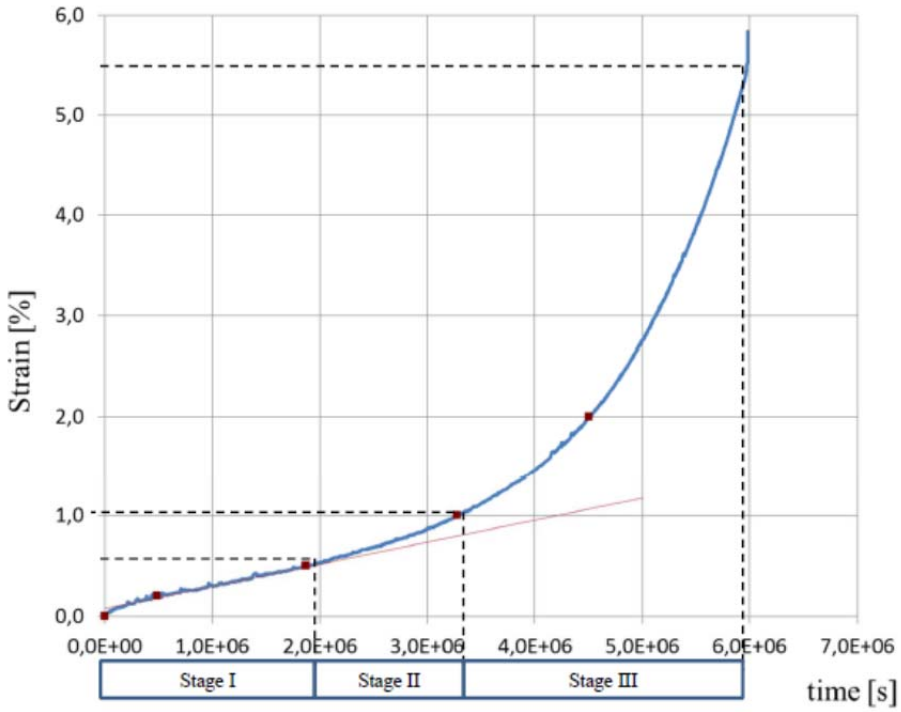

Figure 40: Creep curve of specimen A indicate three characteristic stages of creep

8.3 Stress Relaxation testing

Stress relaxation testing has been performed at 550 ºC at 0.8% applied strain. Like creep it is another method to evaluate the response of In718 under static loading. The deformation is applied and maintained at constant level. The stress drops with time while viscoelastic deformation continues to increase. Figure 41 shows the stress relaxation rate of specimen A and B, that stress relaxation rate of specimen B is smaller than that of specimen A.

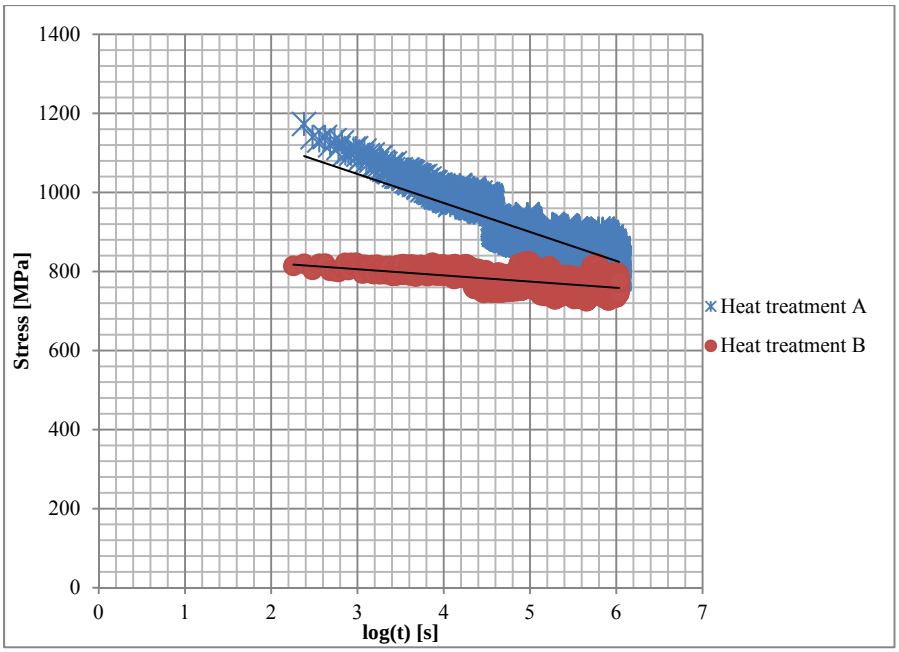

Figure 41: Creep curve of specimen A indicate three characteristic stages of creep

8.4 Hardness Testing

Hardness testing is a simple way of characterizing a material's strength [21]. An indenter consist of different shape is pressed into the surface of the material with a fixed force and the extent of the indentation is measured [21]. The indenter may have a pyramid shape diamond or a steel sphere. The most common hardness tests are [21]:

- Vickers hardness (HV)-pyramid shape indenter
- Brinell Hardness (BH)-circular shape indenter
- Rockwell hardness (HRC)-cone shape indenter

Vickers hardness test has been done in In718 specimens A and B. Figure 42 shows the nomenclature of the indentation obtained from HV test. The formula to calculate the hardness is:

$$HV = \frac{2Fsin136^o}{d^2} = 1.854\ \frac{F}{d^2}$$

Where D is the arithmetic mean of both the diagonals d1 and d2, as shown in the figure 42.

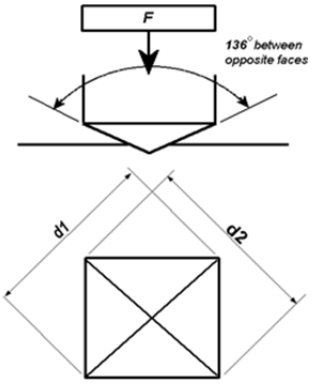

Figure 42: Nomenclature of indentation from HV test [35]

The hardness test is done using a LECO M-400, hardness tester in the Engineering materials laboratory at LiU, as shown in the figure 43.

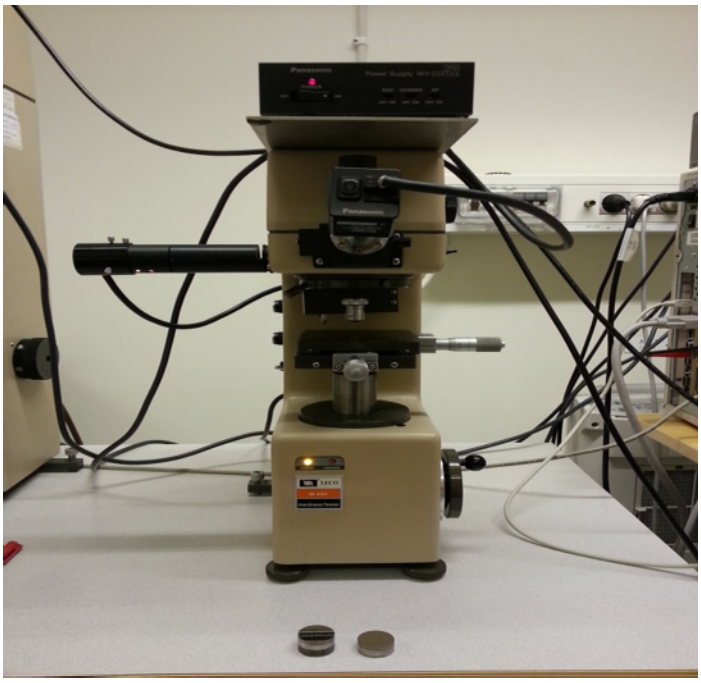

Figure 43: LECO M 400 hardness testing machine

The Vickers hardness test can further be divided into:

- Micro-hardness (10 gm to 1 kg) and
- Macro-hardness (1 kg to 50 kg)

The results of the micro hardness tests are mentioned in the table 10 below as the load selected is 300 gm.

Specimen A				
no.	d1 (µm)	d2 (µm)	mean (µm)	HV
1	34.0	34.1	34.1	479.60
2	34.0	33.9	34.0	481.81
3	34.9	34.1	34.5	468.30
4	34.2	34.5	34.4	470.95
5	34.4	35.1	34.8	460.18
min.	34.0	33.9	34.0	460.18
max.	34.9	35.1	34.8	481.81
mean value	34.3	34.3	34.3	472.17
Specimen B				
no.	d1 (µm)	d2 (µm)	mean (µm)	HV
1	39.2	39.0	39.1	363.81
2	38.8	39.2	39.0	366.03
3	38.6	38.8	38.7	371.86
4	38.9	38.8	38.9	368.20
5	37.6	37.4	37.5	395.18
min.	37.6	37.4	37.5	363.81
max.	39.2	39.2	39.1	395.18
mean value	38.6	38.6	38.6	373.02

Table 10: Hardness testing results for specimen A and B

The calculated mean hardness value for specimen A is approximately 472 and that of specimen B ~ 373. After conversion from Vickers (HV) to Rockwell hardness (HRC) it was found to be ~ 47.5 which is close to the manufacturers given value of 45.4 (See appendix B).

The crystallographic orientation of specimen B is shown in figure 44. The Electron Back Scatter Diffraction (EBSD) technique is used to detect crystallographic orientation. It shows that each and every grain has its own orientation.

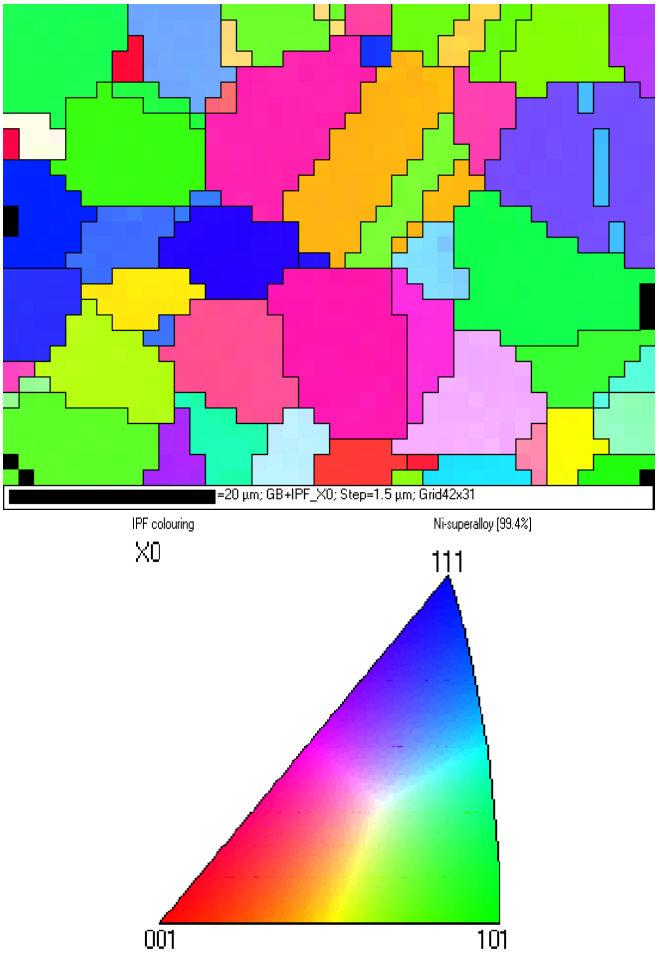

Figure 44: Crystallographic orientation of specimen B using EBSD technique

Conclusion

- Heat treatment as well as constituent elements have potential influence on the mechanical properties of In718.
- The investigation shows that the solution heat treatment of In718 at 1050 ºC, for the time period of 2h caused the complete dissolution of γ′ and partial γ′′ phases.
- The complete dissolution of δ phase at 1050 ºC into the matrix, while at 960 ºC δ phases were observed primarily along the grain boundaries.
- The main strengthening precipitates in In718 are γ′and γ′′.
- The tensile strength of In718 decreased after heat treatment, that is bigger size grains are not good for the strength of In718.
- The creep of In718 increases after heat treatment as the grain size increases
- The stress relaxation results doesn't show distinctive influence of grain size increment
- Nearly 10 times increase in grain size results in deterioration of strength and hardness of In718 .

References

1. R.C.Reed, *The Superalloys* (Cambridge University Press, Cambridge, UK, 2006), p. 372.

2. C.Slama and M.Abdellaoui, *Structural characterization of the aged Inconel 718*, Journal of Alloys and Compounds 306 (2000) 277-284.

3. W. J. Askeland, D.R., Fulay, P.P., Wright, *The Science and Engineering of Materials*, 5th ed. (Global Engineering, 2011), p. 920.

4. Rolls-Royce plc, *The Jet Engine*, 4th edition (Debry, UK: The Technical Publications Department, Rolls-Royce plc, 1992).

5. Siemens Industrial Turbomachinery AB, Inc.

6. Klas Jonshagen, slides on *Gas Turbine dynamic performance,* Siemens Industrial Turbomachinery AB, Inc., presented on Gas turbine course (TMMV12) at Linköping University on October 2013.

7. M. J. Donachie and S. J. Donachie, *Superalloys,* 2nd ed. (OI:10.1361/stgs2002p011; Copyright © 2002 ASM International®; All rights reserved.; www.asminternational.org, USA, 2002), p. 439.

8. W. Sims, C., Stoloff, N., Hagel, *Superalloys II*, October,19 ed. (Intersceince, Wiley, n.d.), p. 615.

9. J. Davis, *Heat Resistant Materials* (1997), p. 591.

10. R. Eriksson, *Thermal Barrier Coatings: Durability Assessment and Life Prediction*, Linköping University, 2013.

11. J. Saarimäki, *The Mechanical Properties of Lattice Truss Structures with Load- Bearing Shells Made of Selectively Laser Melted Hastelloy X*^{TM}, KTH, 2011.

12. http://www.benbest.com/cryonics/lessons.html, website visited on 30 August 2013.

13. http://www.benbest.com , website visited on 30 August 2013.

14. T.M. Pollock, and S. Tin, *Nickel-Based Superalloys for Advanced Turbine Engines: Chemistry, Microstructure, and Properties,* journal of propulsion and power, Vol. 22, No. 2, March–April 2006361 (2006).

15. J. L. Hertzberg, R.W., Vinci, R.P., Hertzberg, *Deformation and Fracture Mechanics of Engineering Materials*, 5th ed. (John Wiley and sons, Inc, New Jersey, 2013), p. 755.

16. D. Gustafsson, *High Temperature Fatigue Crack Propogation Behaviour of Inconel 718*, Linköping University, 2012.

17. M. Durand-Charre, *The Microstructure of Superalloys,* Gordon and Breach Publishers (Amsterdam, 1997), p. 124.

18. M.Dehmas, J.Lacaze, A.Niang, and B.Viguier, *TEM Study of high temperature precipitation of Delta phase in Inconel 718 alloy*, Advances in Material Science and Engineering, Volume 2011, Article ID 940634.

19. L.C.M.Valle, L.S.Araujo, S.B.Gabriel, J.Dille, and L.H.de Al,meida, *The effect of δ phase on the mechanical properties of an Inconel 718 Superalloy*, Journal of materials engg. and performance 1512-Volume 22(5) May 2013.

20. http://www.bodycote.com/services/heat-treatment/solution-and-age/nickel-alloys.aspx, website visited on 30 August 2013.

21. W. F. Hosford, *Materials for Engineers* (Cambridge University Press, New York,USA, 2008), p. 278.

22. ASTM Standard; Designation:E112-12, *Standard test method for determining the average grain size*, ASTM international, West Conshohocken, PA 19428-2959.

23. International Standard ISO 643, *Steels-Micrographic determination of the apparent grain size"*, 3rd edition 2012-12-15, reference no. ISO 643:2012(E).

24. T.Sourmail, P.Opdenacker, G.Hopkin, and H.K.D.H Bhadeshia, *Annealing Twins*, Metals and Alloys, University of Cambridge.

25. http://ocw.mit.edu/courses/materials-science-and-engineering/3-40j-physical-metallurgy-fall-2009/lecture-notes/MIT3_40JF09_lec09.pdf (Website visited on 13th September 2013).

26. S. Dash and N. Brown, *An investigation of the origin and growth of annealing twins,* Acta Metallurgica, Vol. 11, Issue 9, pages 1067-1075 (1963).

27. Y. Jin, M. Bernacki, G.S.Roher, A.D.Rollett, B.Lin, and N. Bozzolo, *Formation of annealing twins during recrystallization and grain growth in 304L austenitic stainless steel, 5th International conference on recrystallization and grain growth,* May 5, (2013) in Sydney, Australia.

28. M. A. Meyers and L.E.Murr, *A model for the formation of annealing twins in F.C.C. metals and alloys,* Acta Metallurgica, Vol. 26, 951-962, Pergamon press, (1978).

29. P. Eklund, *Laboratory exercise in Analytical method in material science*, 2004, Linköping university (Sweden).

30. H. Hogberg and P. Eklund, Lecture slide on *Scanning Electron Microscopy (SEM) and Electron Probe microanalysis (EPMA) Analytical method in material science,* Linköping University (Sweden,) 2013.

31. An-C. Yeh, K.W. Lu, C. Kuo, H.Y.Bor, and C.N. Wei, *Effect of serrated grain boundaries on the creep property of In718,* Materials Science and Engineering,Volume 530, Pages 525–52915, December 2011.

32. W.L.Kimmerle and M.T.Miglin, *Heat treatment of Alloy 718 for improved stress corrosion cracking resistance,* United State Patent, kimmerle et al., June 9, 1989.

33. M.Dehmas, J.Lacaze, A.Niang, and B.Viguier, *TEM study of high-temperature precipitation of Delta phase in Inconel 718 alloy,* Advances in materials science and engineering, Vol 2011, Article ID 940634, 9 pages.

34. T. Dahlberg and Ekberg.A, *Failure Fracture Fatigue An Intoduction* (2002), pages. 356.

35. http://www.gordonengland.co.uk/hardness/vickers.htm, (Website visited on 30th September 2013).

Appendices

Appendix A

The figure below shows the manufactured In718 specimen used for tensile, creep and stress relaxation test. Also parametric 2D drawing is mentioned.

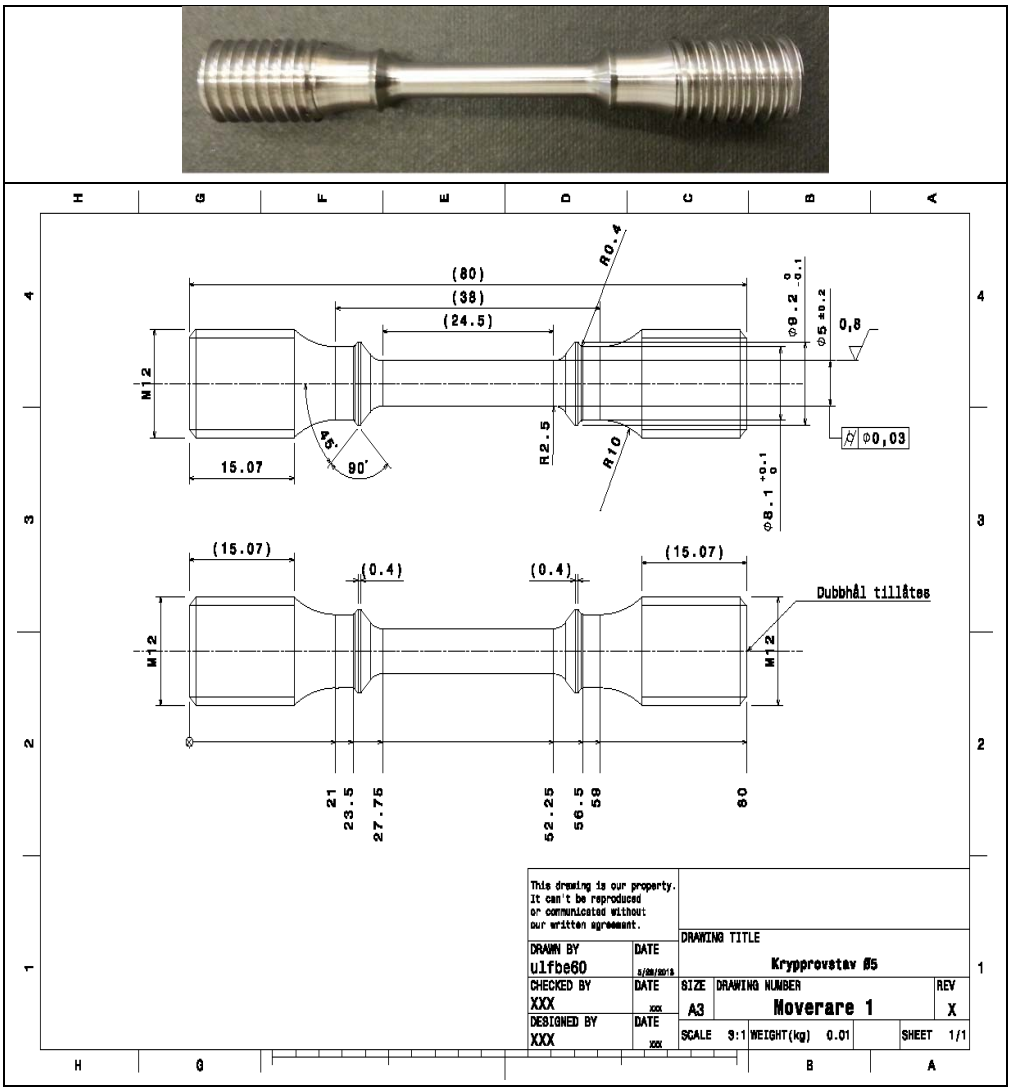

Appendix B

Material certificate data sheet for In718 from the manufacturer.

CERTIFICATE OF LABORATORY TESTS

AS9120 CERTIFIED

SALES

ORD. NO. 4120933

INV. NO 6121573

INDUSTRIAL METALS INTERNATIONAL LTD.
2065 FIFTH AVENUE
PO BOX 306
RONKONKOMA, N. Y. 11779
USA

PHONE: 631-981-1300 / 2300
FAX: 631-981-1339
E-MAIL: INFO@INDUSTRIALMETALS.COM
WWW.INDUSTRIALMETALS.COM

DATE: December 31, 2012

CUSTOMER NAME: GKN AEROSPACE SWEDEN AB

CUST ORD. NO. 45345985-EX

ITEM NO.	SPECIFICATION	DESCRIPTION	QUANTITY	PIECES	NET WT.
1	AMS 5662M	NICKEL 718 BAR, HEAT TREATED TO AMS 5663M (HARDNESS ONLY REPORTED AFTER H/T) 1.00" DIA X 36" MAX LENGTHS MILL: CARPENTER TECHNOLOGY CORPORATION HEAT: 813413	265 LBS	32 PCS	265 LBS

NO.	HEAT NO	C	MN	SI	P	S	CR	NI	MO	CU	CO	AL
1	813413	.03	.09	.10	.007	.0005	18.35	52.50	2.96	.05	.35	.57
		TI	CB	TA	SE	B	BI	FE	PB			
		.97	5.32	.01	< .0003	.004	< .00003	18.42	< .0003			

ITEM NO.	ULT. STRENGTH	YIELD	% ELONG	% R/A	
1	210 KSI	184 KSI	20 %	44 %	HARDNESS: HRC 45.4 MICRO: OK GRAIN SIZE: 9

"THIS PRODUCT CONFORMS TO ALL OTHER TECHNICAL REQUIREMENTS OF THE SPECIFICATION"

AFFIRMED AND SUBSCRIBED TO BEFORE ME THIS 31ST DAY OF DECEMBER 2012

NOTARY PUBLIC

Melanie Hippolito
Notary Public, State of New York
No. 01HI6125408, Suffolk County
Commission Expires April 18, 2013

THE UNDERSIGNED HEREBY CERTIFIES THAT THE FOLLOWING RESULTS WERE OBTAINED FROM LABORATORY TESTS. I CERTIFY THE ABOVE TO BE CORRECT.

INDUSTRIAL METALS INT'L LTD.

CERTIFICATE OF CONFORMITY

IML

INDUSTRIAL METALS INTERNATIONAL LTD.

AS9120
CERTIFIED
2065 FIFTH AVENUE
P.O. BOX 306
RONKONKOMA NEW YORK 11779
PHONE: (631) 981-1300 / 2300
FAX: (631) 981-1339

CUSTOMER NAME: GKN AEROSPACE SWEDEN AB CUSTOMER ORDER NO. 45345985-EX

ORDER NUMBER: 4120933 INVOICE NUMBER: 6121573

ITEM No.	SPECIFICATION	DESCRIPTION	QUANTITY
	AMS 5662M	NICKEL 718 BAR, HEAT TREATED TO AMS 5663M (HARDNESS ONLY REPORTED AFTER H/T)	
1		1.00" DIA X 36" MAX LENGTHS MILL: CARPENTER TECHNOLOGY CORPORATION HEAT: 813413	265 LBS 32 PCS 265 LBS

CERTIFIED that the whole of the materials and/or part detailed hereon conform to the full requirements of the Specifications relative thereto.

AFFIRMED AND SUBSCRIBED TO BEFORE ME THIS

31ST DAY OF DECEMBER 2012

SIGNED Sara Katz
SARA KATZ

Melanie Hippolito
NOTARY PUBLIC

DATE December 31, 2012

Melanie Hippolito
Notary Public, State of New York
No. 01HI6125408, Suffolk County
Commission Expires April 18, 2013